Acta Geologica Polonica, Vol. 62 (2012), No. 2, pp. 143–172
DOI: 10.2478/v10263-012-0007-x

VERSITA

Geochemical and stable isotope patterns of calcite cementation in the Upper Cretaceous Chalk, UK: Direct evidence from calcite-filled vugs in brachiopods

XIUFANG HU[1], CHRISTOPHER JEANS[2] AND TONY DICKSON[3]

[1]*Department of Ocean Science and Engineering, Zhejiang University, Hangzhou 310058, China*
[2]*Department of Geography, University of Cambridge, Downing Street, Cambridge CB2 3EN, UK.*
E-mail: cj302@cam.ac.uk
[3]*Department of Earth Science, University of Cambridge, Downing Street, Cambridge CB2 3EN, UK*

ABSTRACT:

Hu, X-F, Jeans, C.V. and Dickson, J.A.D. 2012. Geochemical and stable isotope patterns of calcite cementation in the Upper Cretaceous Chalk, UK: Direct evidence from calcite-filled vugs in brachiopods. *Acta Geologica Polonica*, **62** (2), 143–172. Warszawa.

The history of research into the cementation of the Upper Cretaceous Chalk of the UK is reviewed. Calcite-filled vugs within the shell cavities of terebratulid brachiopods from the Cenomanian Chalk of eastern England have been investigated by cathodoluminesence imaging, staining, electron microprobe and stable isotope analysis. This has provided the first detailed analysis of the geochemistry of the Chalk's cement. Two cement series, suboxic and anoxic, are recognized. Both start with a Mg-rich calcite with positive $\delta^{13}C$ values considered to have been precipitated under oxic conditions influenced by aerobic ammonification. The suboxic series is characterized by positive $\delta^{13}C$ values that became increasingly so as cementation progressed, reaching values of 3.5‰. Manganese is the dominant trace element in the earlier cement, iron in the later cement. Mn- and Fe-reducing microbes influenced cement precipitation and the trace element and $\delta^{13}C$ patterns. The anoxic series is characterized by $\delta^{13}C$ values that became increasingly negative as cementation progressed, reaching values of –6.5‰. Trace elements are dominated by iron and manganese. Sulphate-reducing microbes influenced cement precipitation and the trace element and $\delta^{13}C$ patterns. Both cement series are related closely to lithofacies and early lithification pre-dating the regional hardening of the Chalk. The suboxic series occurs in chalk which was continuously deposited and contained hematite pigment and limited organic matter. The anoxic series was associated with slow to nil deposition and hardground development in chalks that originally contained hematite pigment but no longer do so, and an enhanced supply of organic matter.

Key words: Chalk; Calcite cement; Trace elements; Stable isotopes; Diagenesis; Microbial influence; Oxia; Suboxia; Anoxia; History.

INTRODUCTION

The Upper Cretaceous Chalk of the British Isles is famous for its whiteness, thickness (800 m) and the magnificent cliffs it forms on the coast of Yorkshire, Kent, Sussex, Isle of Wight and Dorset. Compositionally its sediments are dominated by the low-Mg calcite skeletons of the Coccolithophoridae, usually admixed with minor but varying amounts of foraminifera, bivalves and the calcareous skeletal fragments of other marine invertebrates, as well as the siliceous skeletons of sponges and radiolaria. Traces of continentally de-

rived silicate detritus are also present. Post-depositional processes have modified this sediment to a rock that consists chemically and mineralogically of low-Mg calcite, trace of authigenic clay minerals with bands and nodules of flints. The bulk chalk ranges from a soft very friable rock lacking any appreciable cementation with a porosity of ~40% and a bulk specific gravity of ~1.6, such as is typical of southeast England, to a hard micritic limestone with little porosity (10% or less) and a bulk specific gravity of 2.3–2.6 that is found in Yorkshire, Lincolnshire, southwest England and Northern Ireland.

For well over a century there has been much scientific interest in how the Chalk has managed to remain in a soft friable essentially uncemented state, whereas in other places it has been cemented into a hard fine-grained micritic limestone. This is of particular interest to those who deal with the Chalk as a water or hydrocarbon reservoir (Hardman 1982) or with its engineering properties (Mortimore 2012 in press). The problem with the Chalk is the exceptionally fine grain of the original sediment, which has meant that attempts to study the petrography and geochemistry of the intergranular cements by electron microscopy and electron microprobe analysis have not met with great success.

The paper reviews the history of geochemical and related research into the calcite cements of the Chalk. It then describes and discusses the trace element and stable isotope patterns in calcite cement filling vugs within the shell cavities of terebratulid brachiopods from the Cenomanian Chalk of eastern England. Evidence is put forward that these patterns are related to early lithifications that are widespread in the Chalk, such as hardgrounds (Jukes-Browne and Hill 1903, 1904), associated with large ammonites (Wright 1935; Jeans 1980) and nodular chalks and marls (Jukes-Browne and Hill 1903, 1904), and not to the late cements responsible for regional hardening of the Chalk.

PREVIOUS RESEARCH

Jukes-Browne and Hill (1903, 1904) recognized the full range of lithofacies in their monumental review of the Chalk of England. Chalk rocks, nodular chalks and more and less hard normal white chalk were all differentiated and their regional and stratigraphical distributions were established within the zonal scheme of the time. Missing were the detailed observations that would have allowed them to deduce that the chalk rocks and nodular chalks originated at or just below the seawater/sediment interface, whereas the hardening of the white chalk was a much later diagenetic event. It was left to Bromley's classic studies (Bromley 1967, 1968) on the Chalk Rock and associated lithologies to demonstrate that they represented seafloor lithification with convincing evidence of encrusting and boring organisms.

Häkansson *et al.* (1974) recorded that the hardground cements (i.e. chalk rock of Jukes-Browne and Hill, 1903) of the Maastrichtian Chalk of NW Europe were low-Mg calcite and that this caused a porosity reduction of 5–15% depending on the extent to which the original chalk prior to lithification had undergone compaction. The cement occurred as euhedral calcite crystals in intergranular and intragranular voids and as overgrowths on coccolith calcite. In hardgrounds formed during the earlier stages of diagenesis, cementation preceded most compaction and dissolution of skeletal aragonite and silica. These early low-Mg calcite cements were often enriched in Mg compared to the uncemented chalk (Clayton 1986; Hancock 1975; this paper, see later): however the presence of *Inoceramus* prisms with their high Mg content (3500–15735 ppm, Jeans *et al.* 1991; Table 2) may obscure this slight enrichment.

The next step in the understanding of this early "hardground" lithification came from the Cenomanian chalks of east England. Jeans (1980) demonstrated that cementation in five types of early lithification resulted from the precipitation of calcite enriched in Fe and that this was associated with the widespread dissolution of ferric hydroxide present in the sediment. It was argued that the precipitation of the calcite cement and dissolution of the ferric hydroxide were under microbial control.

Early calcite cementation and lithification is associated with Paramoudra flints, vertically extensive tubular flints that are characteristic of certain levels in the Chalk (Bromley *et al*. 1975; Mortimore 2011). The cementation and lithification is restricted to the tubular mass of chalk surrounded by the flint; it is related also to a glauconite- or pyrite-stained *Bathichnus* burrow at the centre of the tubular chalk mass which extends the full length of the flint. Clayton (1986) has estimated the calcite cement within a paramoudra flint from the Campanian of Norfolk to have an average Mg content of 1536 ppm and stable isotope values of $\delta^{18}O$ –11.9‰ and $\delta^{13}C$ 1.13‰ (V-PDB). It was suggested that cementation was affected by sulphate-reducing bacteria which contributed 10% of the cement, the rest coming from marine sources.

Ideas on the regional hardening of the Chalk were reported in the geological literature from the second half of the nineteenth century and onwards (Hancock 1963). The exceptionally hard chalks of Northern Ireland overlain by a thick basalt pile were a topic of much interest – ideas ranged from baking by the volcanic pile to the possibility that the Irish Chalk had a higher proportion of aragonite in the original sediment (Hancock 1963). In

Yorkshire and southwest England, the association of faulting and high dips was thought to be related to the general hardening (Mimran 1977, 1978).

The first detailed investigation of the petrography of hardened chalk was carried out by Wolfe (1968) on the Irish Chalk using transmission electron microscopy combined with determination of the degree of sediment and fossil compaction prior to lithification. Wolfe recognized two lithification phases: (1) an early one, little affected by compaction, associated with sparry calcite infilling the originally empty moulds of aragonitic and siliceous fossils (equivalent to the chalk rocks of Jukes-Browne and Hill 1903 and the hardgrounds of Bromley 1967. 1968); and (2) a later phase occurring after 15–25% compaction of foraminifera tests (15–31% compaction of microfossils) caused by widespread cementation by calcite precipitated from solutions derived from the pressure solution of the chalk – this is the regional hardening recognized by Jukes-Browne and Hill (1903) in their normal hard white chalk. Wolfe concluded that recrystallization played only a minor role. Maliva and Dickson (1997) have extended this investigation into the Irish Chalk with stable isotopes ($\delta^{18}O$, $\delta^{13}C$) and trace element analysis using laser ablation isotope analysis combined with microprobe analysis to provide details of the chemical variations in the cements. These authors concluded that: (1) cementation and recrystallization took place as the result of deep burial beneath a 2–3 km pile of Tertiary lavas at a maximum burial temperature of ~105°C; and (2) the cement was derived from the pressure solution of the chalk and was precipitated under low water-rock ratios in an environment of either marine or mixed marine-meteoric porewater.

The discovery in the late 1960s of commercially important hydrocarbon accumulations (including the giant Ekofisk Field) within chalk reservoirs in the Norwegian and Danish sectors of the North Sea and more recently in the UK sector has provided major impetus to the study of chalk diagenesis. Of particular interest has been the complex relationship between depositional lithofacies, compaction, consolidation, cementation, pressure dissolution, fracturing and the porosity and permeability character of the chalk (Oakman and Partington 1998). Scholle (1974) surveyed the compaction, cementation history and stable isotope ($\delta^{18}O$, $\delta^{13}C$) patterns for the hardened chalks of Northern Ireland and Yorkshire, the soft chalks of southeast England and Denmark, and the chalks from the Ekofisk Field of the North Sea. The low porosity (5–10 %) highly cemented chalk of Northern Ireland exhibit the greatest degree of compaction and the lowest $\delta^{18}O$ values (average –5.6‰). The Yorkshire chalks have suffered moderate compaction and cementation, their porosities average 18% and their $\delta^{18}O$ values averaging –4.0‰. The practically uncemented chalks of southeast England and Denmark have the highest porosities (40–45%), show little or no evidence of compaction and have highest $\delta^{18}O$ values (average –2.9‰). The Ekofisk chalks display a very different pattern and this was unrelated to present burial depths. Porosities ranged from 2% to 43%, reflecting different degrees of cementation, whereas the $\delta^{18}O$ values showed little variation, averaging –0.4‰. Scholle's preferred interpretation for the onshore chalks was the replacement of the original marine porewaters by meteoric water, then burial under varying degrees of hydrothermal heating – the greatest in Northern Ireland, less in Yorkshire, and little or none in southeast England and Denmark. Subsequent studies have given little support to the hydrothermal heating hypothesis (Mimram 1978, Maliva and Dickson 1997). Mimram (1978) supported the idea of the replacement of the original porewaters by meteoric water in the Irish and Yorkshire chalks, whereas the most recent and comprehensive study (Maliva and Dickson 1997) of the Irish Chalk concluded that the porewaters were essentially marine, perhaps with a minor meteoric influence. Scholle (1974) considered the Ekofisk chalk to have undergone diagenesis within its own marine porewaters, a conclusion that is in general agreement with the most recent studies (Maliva and Dickson 1992; Egeberg and Saigal 1991; Maliva *et al.* 1995) on various chalk fields in the North Sea. In the North Sea chalk reservoirs particular attention has been paid to the detailed relationship between microlithofacies and the diagenetic control of porosity. For example, Maliva and Dickson (1992) have unravelled the complex interrelationship in the Cretaceous / Tertiary chalks of the Eldfisk Field.

The relationship between the cementation of the chalk and the calcite veins that crosscut it has been a topic of considerable research. Onshore Mimram (1977, 1978) and Jeans (1980) have considered the possibility that the vein calcite represented the cement responsible for the general cementation of the Chalk of Ireland, Yorkshire, Dorset and Northern Ireland. For the North Sea chalks, Watts (1983) has considered the timing and development of fractures. Taylor and Lapré (1987), Jensenius (1987), Jensenius *et al.* (1988), Jørgensen (1987) and Jensenius and Munksgaard (1989) concluded that the healing of the fractures by calcite precipitation occurred during phases of ascending hot water. However, Egeberg and Saigal (1991) have found evidence in the cement of the chalk matrix and in the healed fissures that the calcite cement originated locally from pressure dissolution processes of the chalk matrix in a closed or semi-closed diagenetic system. A similar conclusion was reached by Maliva *et al.* (1995) in their study of the chalk reservoir in the

Machar Field (UK North Sea). Dolomite is a minor relatively late diagenetic cement in the North Sea Chalk (it occurs also in parts of the French Chalk, but not in the onshore chalks of the UK). A detailed study (Maliva and Dickson 1994) of its origin in the Eldfisk, Tor, Dan and Machar oilfields suggests that the Mg was derived from the neomorphism of high-Mg calcite to low-Mg calcite and that the dolomite was precipitated in modified marine porewaters.

The role of the increasing deformation on the hardness and composition of the Middle (Turonian) and Upper ('Senonian') Chalk associated with post-Cretaceous steep, asymmetrical east-west folding in southern England (Surrey; Isle of Wight; Dorset) and Yorkshire has been investigated by Mimran (1975, 1977, 1978), making comparison to his own findings (ideas) on the unfolded chalk of Northern Ireland (Mimran 1978) which differ significantly from those of Wolfe (1968) and Scholle (1974). Mimran (1977, 1978) modelled the effects of increasing deformation using measurements of acid insoluble residue, bulk specific gravity (intact dry density), concentration and distortion of calcispheres (assumed to be originally spherical in form), values of various elements (Sr, Mg, Ti, Ba), and stable isotopes ($\delta^{18}O$, $\delta^{13}C$) in bulk chalk calcite, and microfabric analysis. Isotope evidence suggested that the hardening process in southern England, Yorkshire and Northern Ireland all took place with porewaters of differing Sr contents but of meteoric origin. In the hard chalks of Dorset four stages of alteration in low Sr meteoric porewaters related to increasing deformation were postulated. Stage 1 involved compaction, lithification, pressure dissolution at intergranular contacts, the reprecipitation of low-Sr calcite as spar in calcispheres and foraminifera and as overgrowths on other calcitic bioclast grains. This involved an increase in bulk specific gravity of ~1.75 to 2.38 and a total volume reduction of 25–30%. Stage 2 involved an increase in acid insoluble residue by $CaCO_3$ dissolution under high pore-fluid pressure; this resulted in the preferential removal of the calcite overgrowths as well as general loss of $CaCO_3$ from the coccolith calcite, resulting in enhanced overall Sr content. This increased the total volume loss to 55% and bulk specific gravities to between 2.38 and 2.43. Stage 3 involved $CaCO_3$ loss under extensive confining pore-fluid pressure. Further compaction brought the total volume loss to 95%, with bulk specific gravities ranging from 2.4 up to 2.6 and a marked reduction in bulk Sr values. Stage 4 involved (a) further loss of $CaCO_3$ but without further compaction as the fine bioclastic material between the closely packed spar-filled calcispheres (average 70 μm diameter) was preferentially dissolved; (b) an increase in acid insoluble residue; (c) a reduction in Sr contents as the last remaining coccolith material was lost; and (d) a reduction in bulk specific gravity. Regional variations between Dorset, Isle of Wright and Surrey (Guildford) are related to different overburden pressures of the overlying Tertiary sediments, whereas in Yorkshire and Northern Ireland an early phase of externally derived Sr-rich $CaCO_3$ cement was introduced before the crushing of microfossils. This prevented further compaction and was accompanied by the recrystallization of ~20–30% of the original bioclastic particles with the enhancement of their Sr contents. Hardening of the Yorkshire Chalk preceded folding. The Irish Chalk is similar to the Yorkshire Chalk in that it has been affected by an early phase of externally derived $CaCO_3$ cement with low Sr content (20 ppm) derived from meteoric porewater during the Chalk's exposure prior to burial beneath the 2–3 km thick basalt lava pile.

GEOCHEMISTRY OF CALCITE CEMENTS IN THE CENOMANIAN CHALKS OF EASTERN ENGLAND

The general absence of large permanent pores or voids in the Chalk during its diagenesis has meant that sufficiently large crystals of calcite cement for detailed geochemical analysis have not developed. Locally there are certain hardgrounds where large mouldic voids after aragonitic fossils are present and they may contain calcite spar (Häkansson *et al*. 1974). Such examples are rare even in hardgrounds and they are absent from other chalk lithologies. An alternative source of voids in the Chalk are thick-shelled, compaction-resistant terebratulid brachiopods when they have been buried with their valves in place without their shell cavity being filled completely with sediment. When this has happened the original void

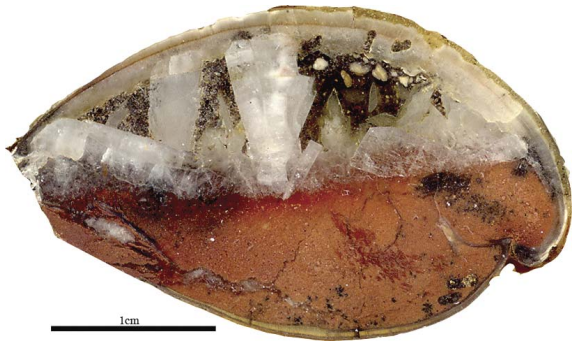

Text-fig. 1. Barytes and calcite crystals in the shell cavity of terebratulid brachiopod T1, Belchford Member (Ferriby Formation), Speeton. The best preserved calcite cement forms the roof to the vug. Large crystals of barytes have grown on the chalk floor from solutions rich in sulphate and barium at the margin of the sulphidization zone that cuts across the pink and red bands in the Ferriby Formation

has been filled with calcite cement and sometimes other minerals (Text-fig. 1). Examples are rare. In spite of the availability of large number of brachiopods from the Cenomanian chalks of eastern England to choose from, only 18 were suitable for detailed investigation. The presence of vugs could be identified by careful examination through the translucent shell. All came from coastal cliff exposures, possibly reflecting the less favourable collecting conditions of the inland exposures. The calcite crystals in these vugs have provided for the first time a direct and detailed record of the cementation history of the Chalk.

The locations in east England mentioned in the text are shown in Text-fig. 2. The regional stratigraphy and the stratigraphical terms used in the text for the Upper Albian and Cenomanian Chalks in eastern England are displayed in Text-fig. 3, formation and member names respectively are those of Wood and Smith (1978) and Jeans (1980). The horizons of brachiopods (T1–T11) and the subdivisions of the Red Chalk and Ferriby Formations at Speeton used by Mitchell (1995, 1996) are shown in Text-fig. 4; however, the base of the Ferriby Formation has been placed at the top of Mitchell's (1995) Weather Castle Member as this is a better lithological match to the sequences to the south

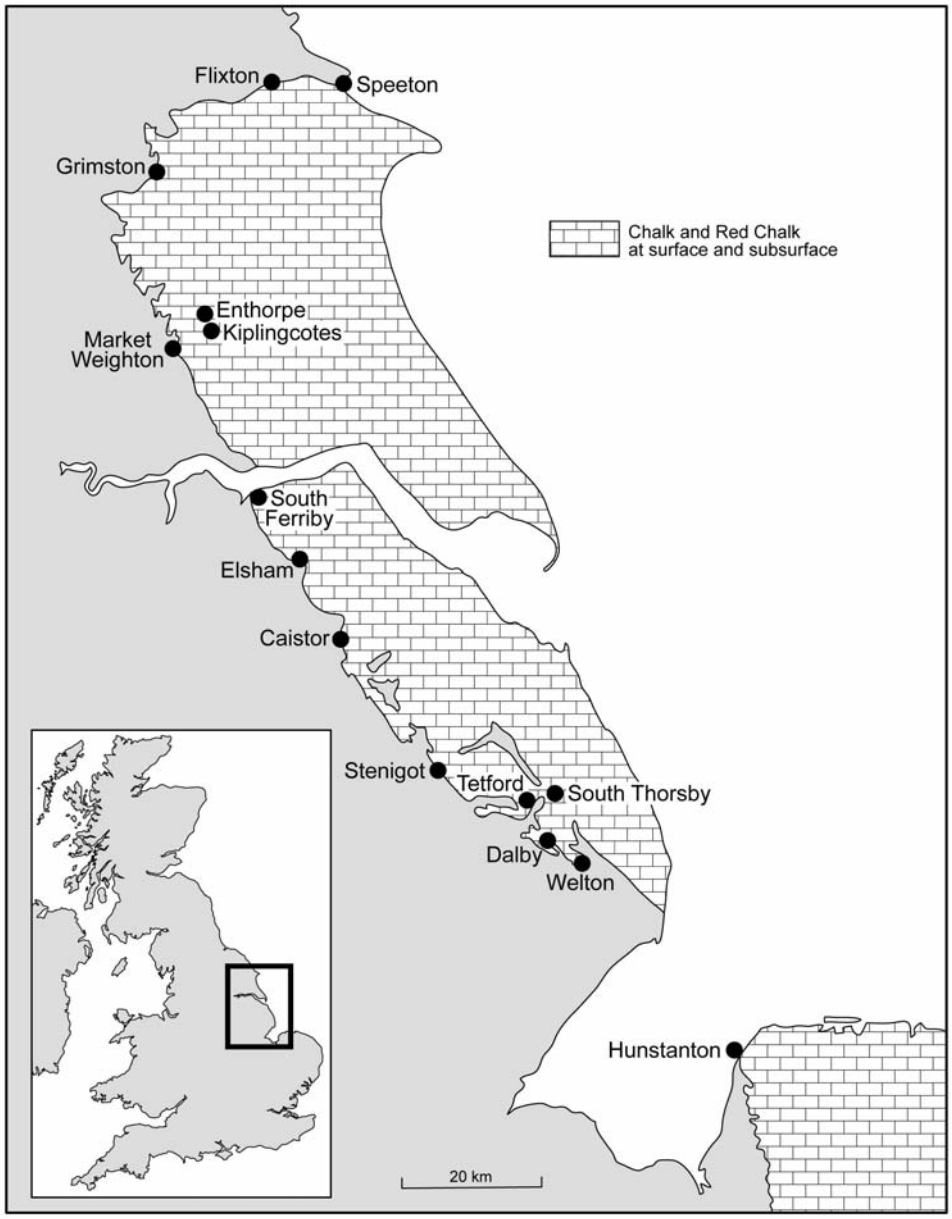

Text-fig. 2. Distribution of Chalk and Red Chalk at the surface and subsurface in eastern England. Locations mentioned in the text are shown

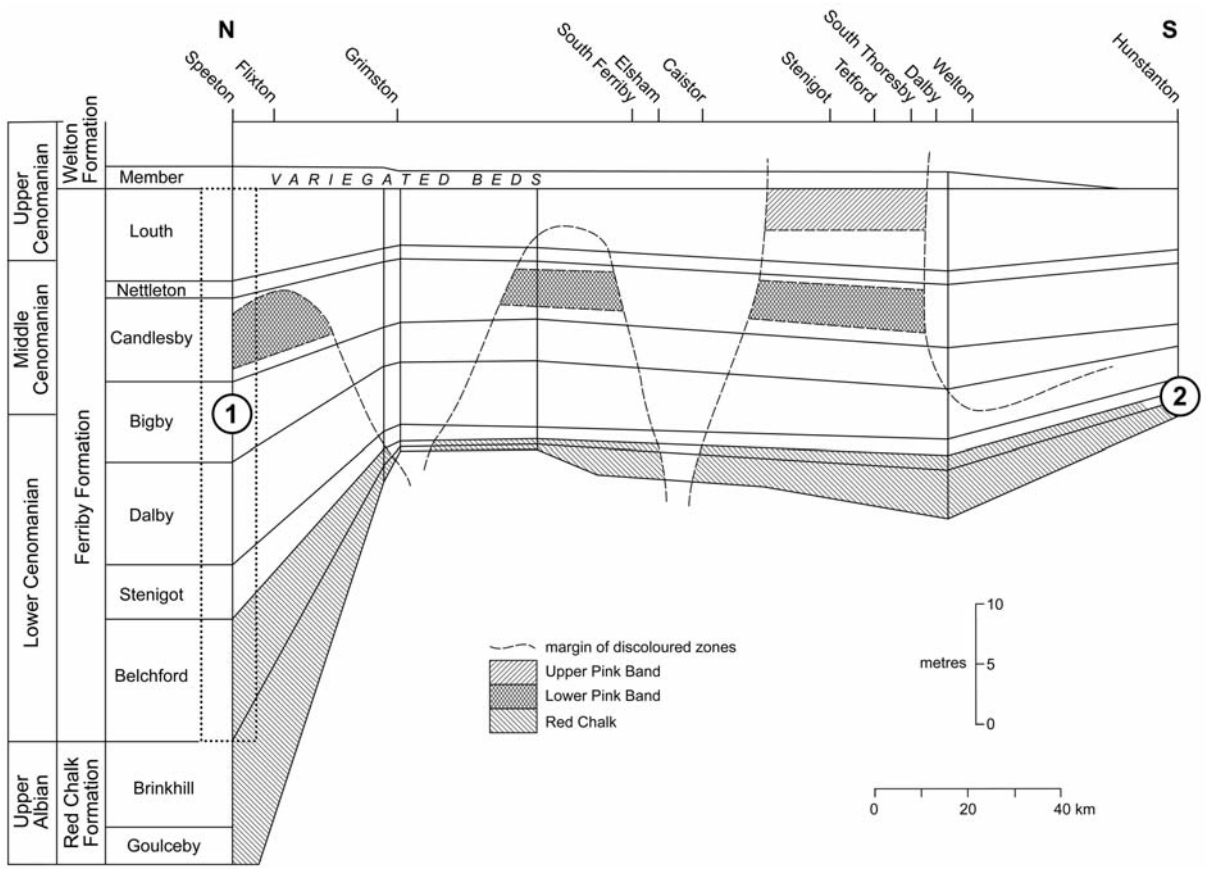

Text-fig. 3. Horizontal section through the Red Chalk, Ferriby and basal Welton formations in eastern England based on Bower and Farmery (1910) and Jeans (1980). The extent of the main bands of red and pink chalk and the zone of discolouration are shown. The Paradoxica Bed marks the top of the Belchford Member. Location and stratigraphical distribution of the terebratulid brachiopods investigated from Speeton (1) and Hunstanton (2) are shown

(Jeans 1980). Variegated Beds (Wood *et al.* 1997) is preferred for the coloured marls and marly chalks at the base of the Welton Formation instead of Plenus Marls or Black Band. The complex relationship in the Speeton Cliffs between the coloured chalks and the Red Chalk and Ferriby Formations and the zones of sulphidization is illustrated in Text-fig. 5. The horizons of brachiopods (T12–T16) from Hunstanton are shown in Text-fig. 6.

ANALYTICAL METHODS

Thin section preparation

Terebratulids were cleaned using acetone and cast in resin. The casts were cut with an annular saw (blade 0.8 mm thick) into several thin slices approximately 1 mm thick. Each of the terebratulid slices was temporarily mounted onto a glass slide using wax and its upper surface was ground flat. This surface was later mounted permanently onto a second glass slide using Norland optical UV adhesive 61. After the adhesive solidified, the first glass was removed by melting the wax to about 60°C. The revealed surface was ground and polished.

Two representative slices from each terebratulid were selected for $\delta^{13}C/\delta^{18}O$ analysis and electron probe microanalysis respectively. Normal light petrography was observed using a Zeiss Axioplan petrological microscope equipped with a Cannon PowerShotA640 camera.

Cathodoluminescence

The polished thin sections were examined using an in-house cathodoluminescence unit (cold cathode) connected to Nikon Microphot microscope with ×2 and ×10 objective lenses. An accelerating potential of ~26 kV generated a gun current of 450 to 600 mA with an air chamber pressure of 0.01 to 0.05 Torr. Cathodoluminesence (CL) images were captured digitally using an Optronics digital microscope camera and processed using image capture software MagnaFIRE developed by Optronics. Exposure time commonly varied between 3 and 20 seconds.

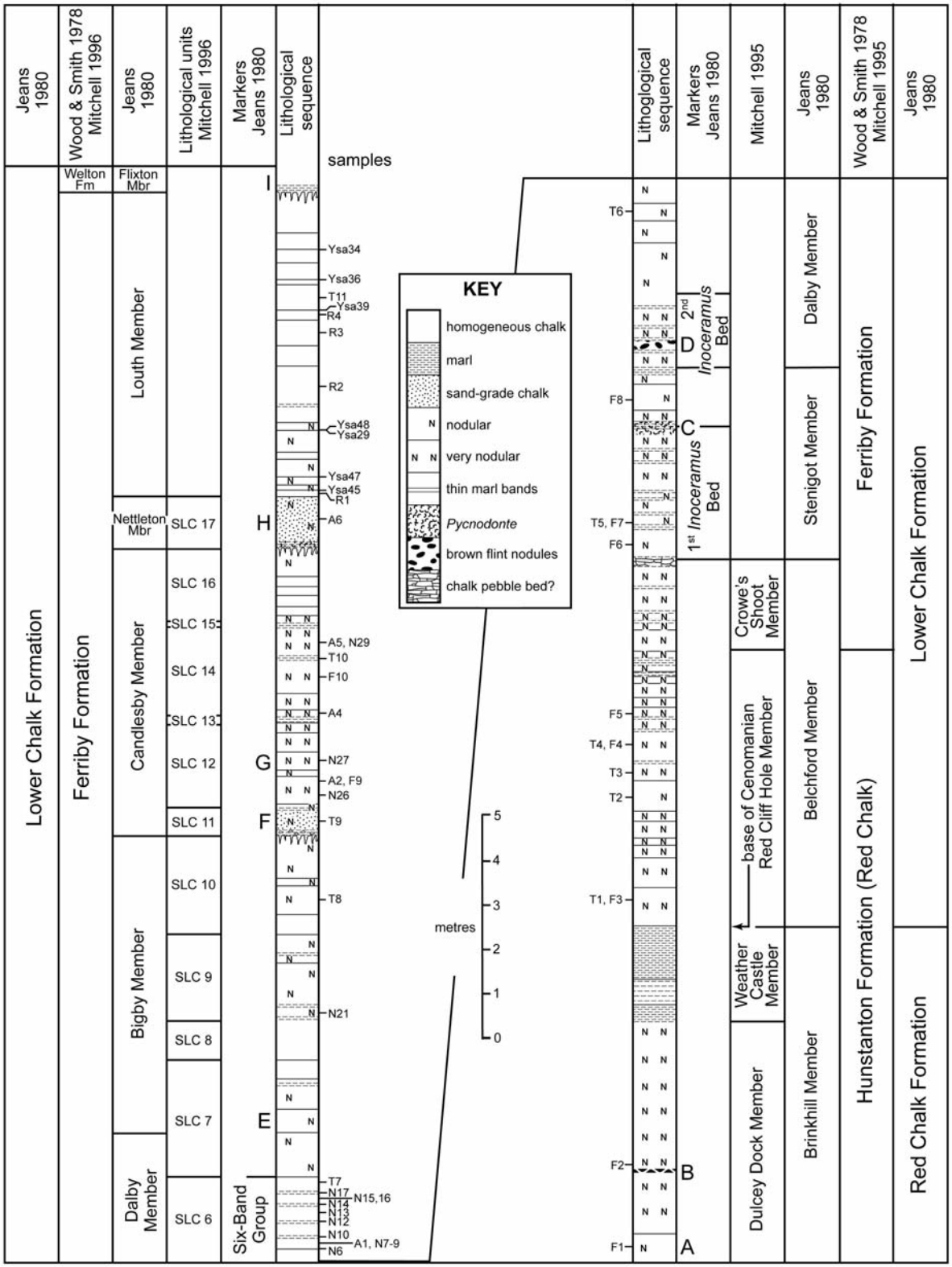

Text-fig. 4. Lithostratigraphy of the upper part of the Red Chalk Formation and the Ferriby Formation at Speeton, Yorkshire, based upon Jeans (1980, fig. 16). A – *Inoceramus*-rich horizon. B – Breccia-nodule Band. C – Band of abundant *Pycnodonte*. D – Brown Flint Band. E – Lower *Orbirhynchia* Band. F – Grey Bed. G – Upper *Orbirhynchia* Band. H – Nettleton Stone. I – Variegated Beds. Stratigraphical levels of the terebratulid brachiopods (T1–T11) and other samples investigated in a closely related research project are indicated. The various schemes of lithological subdivisions used by Mitchell (1995, 1996) are shown

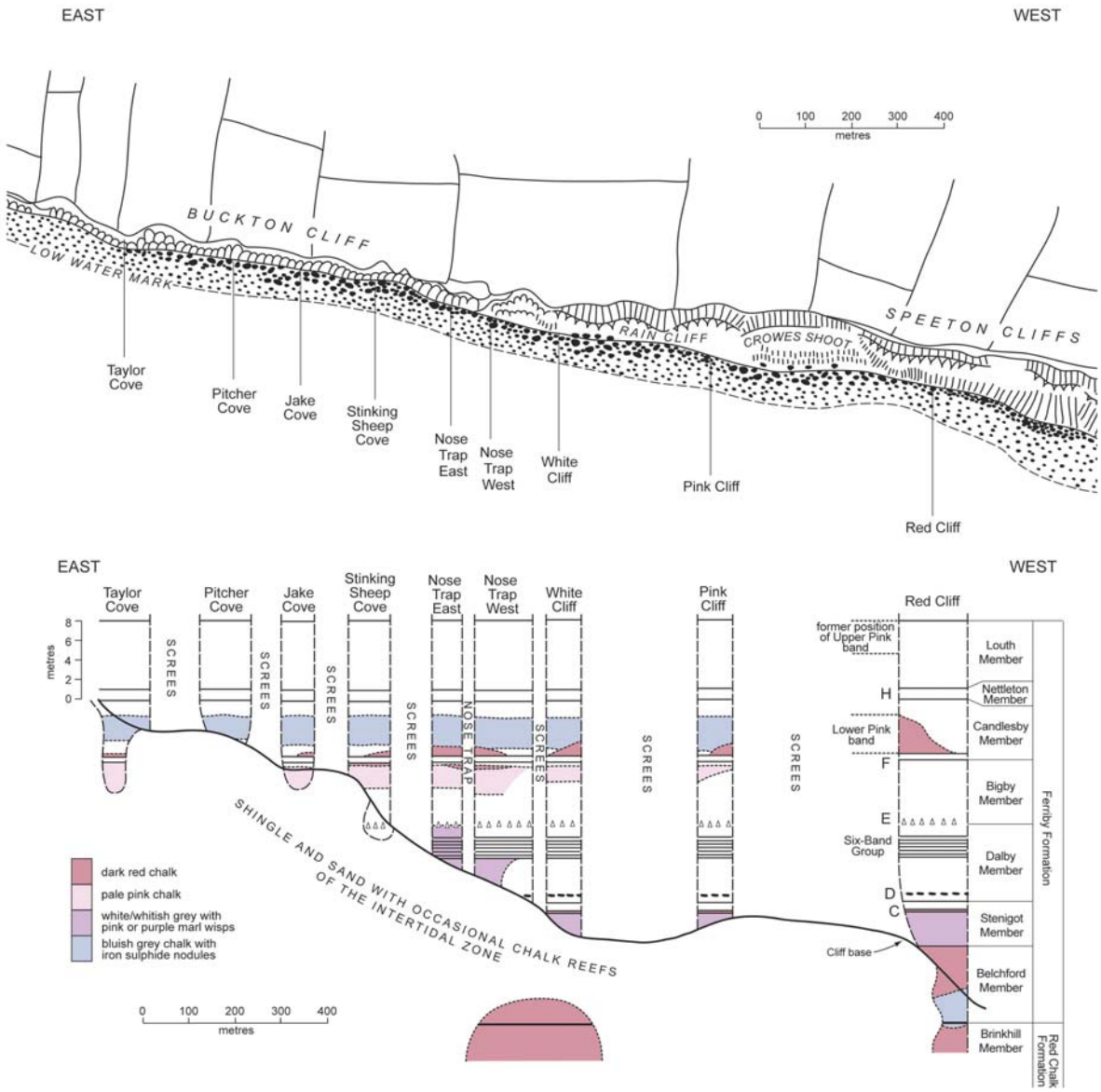

Text-fig. 5. Horizontal sections of the Ferriby Formation and upper part of the Red Chalk Formation at various locations in the cliffs at Speeton and Buckton, Yorkshire. C – Band of abundant *Pycnodonte*. D – Brown Flint Band. E – Lower *Orbirhynchia* Band. F – Grey Bed. H – Nettleton Stone. The distribution of red, pink and purple strata and zones of discoloured chalk with iron sulphide crystals and nodules are shown

Staining

The thin sections were stained with alizarin red S and potassium ferricyanide to display the distribution of ferrous iron in the calcite cements (Dickson 1965, 1966).

$\delta^{13}C/\delta^{18}O$ analyses

Based on the calcite cement zonal sequences displayed on CL images, isotope samples were collected under a low-magnification microscope using a needle and fine brush. 20–50 μg of calcite powder was extracted and one to three samples were taken of calcite cement from single terebratulid sections, depending on size and zonation. Carbon and oxygen isotope analyses were performed using a Micromass Multicarb separation system connected to a VG Prism II stable isotope ratio mass spectrometer housed in the Godwin Laboratory for Palaeoclimate Research, Department of Earth Sciences, the University of Cambridge, U.K. Each sample batch was accompanied by 10 reference carbonate and 2 'control' samples. The results are reported as deviations from the international standard V-PDB (‰). Precision was measured as better than 0.06 ‰ for $\delta^{13}C$, and better than 0.08 ‰ for $\delta^{18}O$.

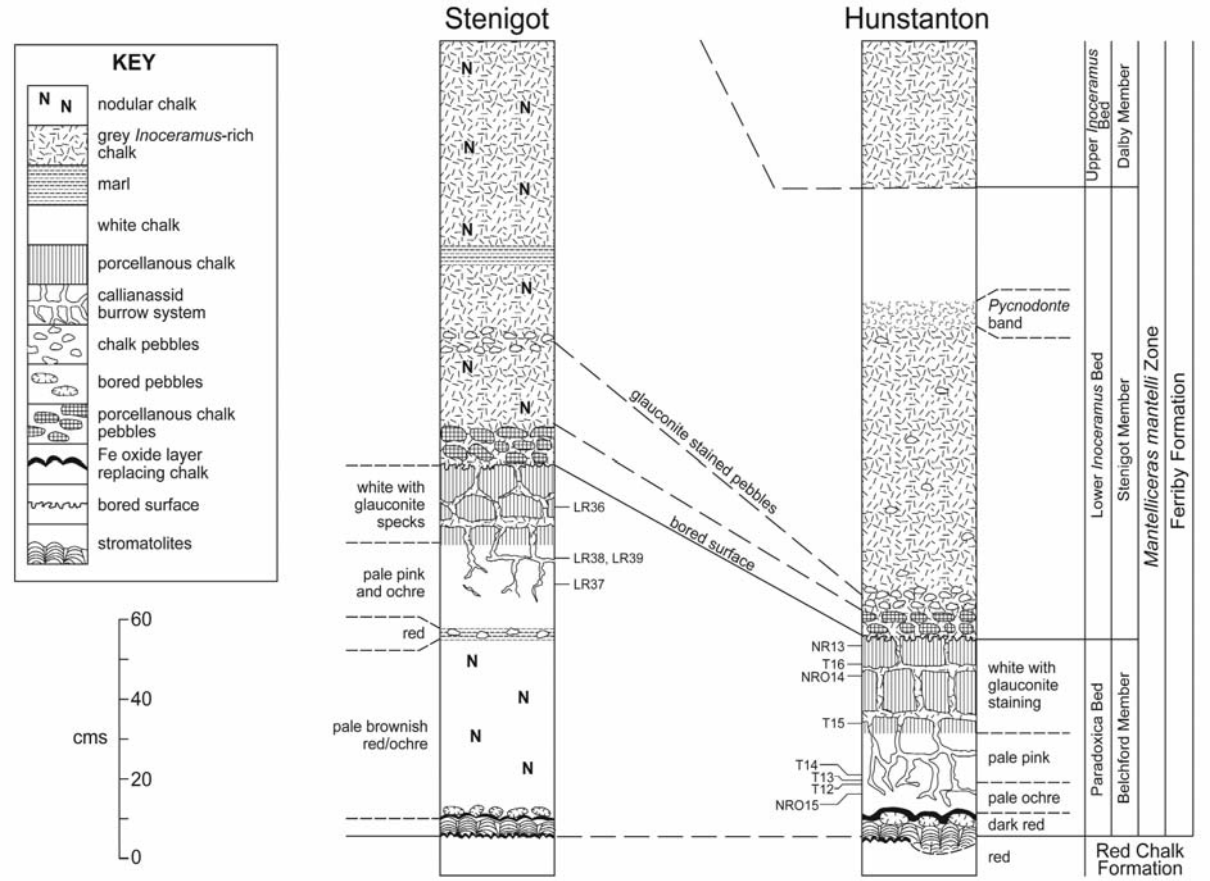

Text-fig. 6. The lithostratigraphy of the basal part of the Ferriby Formation at Hunstanton (Norfolk) and Stenigot (Lincolnshire). Stratigraphical levels of terebratulid brachiopods T12–T16 and other samples (NOR, LR) analysed in a closely related research project are indicated

Electron Probe Microanalysis

Electron probe microanalysis (EPMA) was used to detect the concentration of trace elements in the calcite cement crystals. Fe, Mg, Mn and Sr concentrations were determined using a Cameca SX100 electron probe microanalyzer. Wavelength dispersive analysis was conducted on carbon-coated thin sections; accelerating potential = 15 kV; beam current = 15 nA; beam diameter = 20 μm. Detection limits for Sr, Fe, Mn = ~300 ppm; for Mg = ~90 ppm. Quantitative line analysis was done along the growth direction of calcite crystal in each sample. CL photos were taken after analysis as each analyzed point was visible and its relationship to calcite zonation was recorded.

Burial Curves

The burial and palaeotemperature curves for Speeton and Hunstanton have been derived from data in Downing *et al.* (1985), Kirby *et al.* (1985), Green (1989), Bray *et al.* (1992), Holliday (1999), Hopson (2005) and Hopson *et al.* (2008) using Schlumberger's software PetroMod 11 ID Express.

VOIDS FILLED WITH CALCITE CEMENTS INSIDE TEREBRATULID BRACHIOPODS

The brachiopods investigated are numbered T1–T16 and the beds from which they were collected are shown in Text-fig. 3 (T1–T11) and Text-fig. 6 (T12–T16). The specimens from Speeton (T1–T11) have been identified by comparison with Mitchell's (1995) description of the terebratulids from the Hunstanton Red Chalk and Ferriby Formations at this location. Those from Hunstanton (T12–T16) are part of the collection of C.V. Jeans and I.M. Platten described in Peake and Hancock (1961), their identification was based upon Sahni (1929). All were well preserved with both valves intact and tightly closed.

The cement-filled vugs represent spaces that had not been filled with chalk sediment when the brachiopod was buried (Text-fig. 7). Originally the floor

of each void was flat representing the contact between the porewater of the entombing sediment and the chalk sediment that had managed to find its way into the shell cavity. The roof of the voids was a section of the internal surface of the brachiopod's dorsal and ventral valves. Depending upon the orientation of the brachiopod when it was buried and the amount of sediment filling the body space, different areas of the valves have acted as the roof. A few of the brachiopods had been slightly affected by compaction (Text-fig. 7).

These brachiopods had probably the misfortune of having been buried alive in chalk sediment. One can imagine the situation – their quick and catch abductor muscles snapped their valves shut before sediment could enter the mantle cavity and damage their lophophores (Rudwick 1970). Only after death, no doubt at least after some days, did these muscles rot and a trickle of chalk sediment find its way in between the tightly fitting valves to fill the shell cavity to various extents, leaving a void filled by porefluid from which the cement crystals were precipitated.

CALCITE CEMENT OF THE BRACHIOPODS

The main features of the cement from the shell cavities are described from five examples, terebratulid brachiopods T1, T4, T11, T12 and T16. CL imagery shows that a considerable number of zones may be present, ranging from only a few (T1) to many (T16). The labelling of these zones is specific to each individual brachiopod with two exceptions. Zone A refers always to the earliest cement, if present, which is non-luminescent. The same scheme of zones has been applied in brachiopod T12 and T16 where there is a good match.

Terebratulid T1 (*Concinnithyris subundata* (J. de C. Sowerby)) is from near the base of the Belchford Member (Ferriby Formation) at Speeton (Text-fig. 4). The brachiopod was buried upside down in a red chalk sediment with its dorsal valve beneath (Text-figs 1, 7). The original void was extensive, dominating the ventral half of the shell cavity; its floor was red chalk sediment and the roof was the ventral valve. There are two phases of mineral deposition. The first was calcite cement, which is best

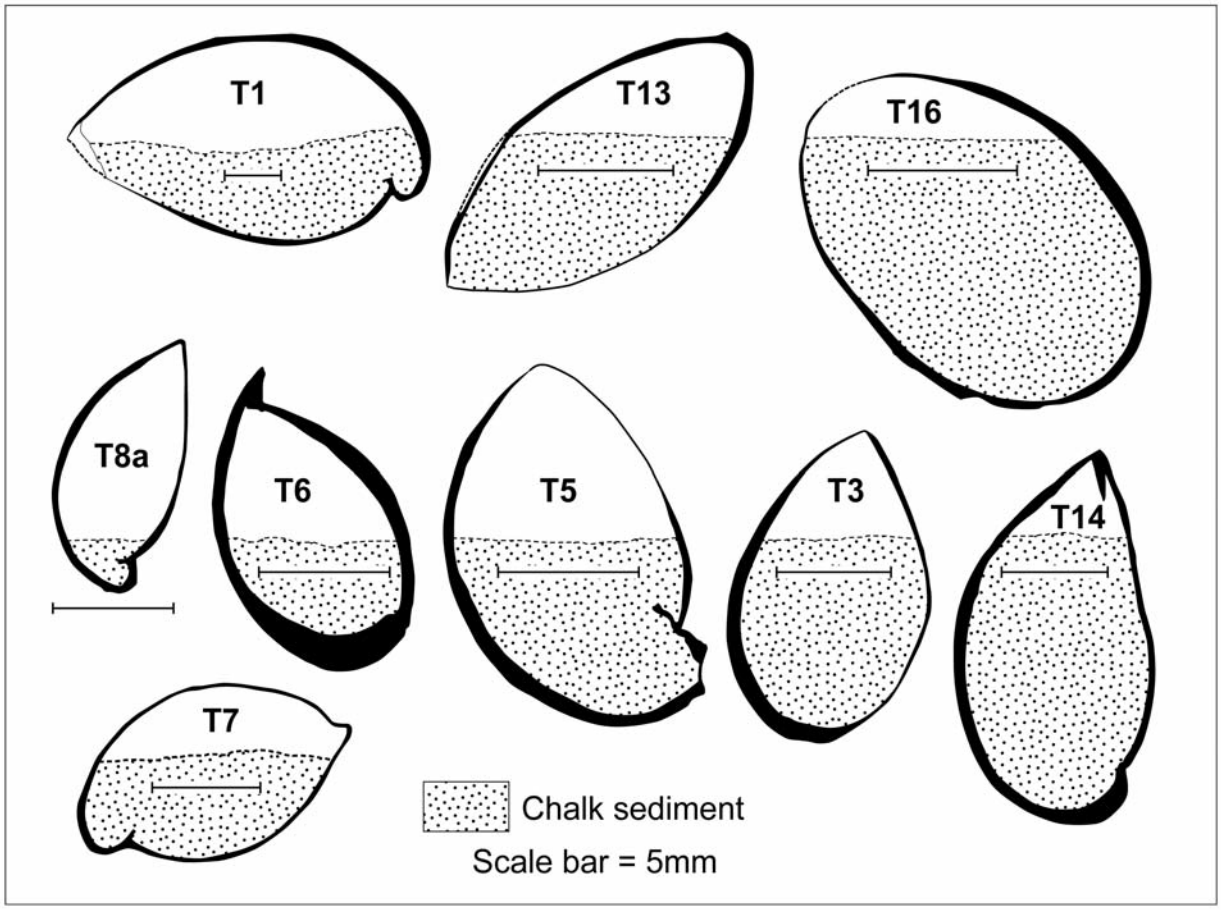

Text-fig. 7. Slices of terebratulid brachiopods from Speeton and Hunstanton showing the orientation of burial and the extent of the calcite-filled vugs in their shell cavities. Brachiopods T6, T7 and T14 have been crushed by compaction

preserved in the upper part of the void where it has seeded on the inside of the ventral valve. The second and later phase was the growth of large baryte crystals from the floor of the void (Text-fig. 1): this is related to the penetration during late diagenesis of sulphate-rich pore-fluids in zones that cross-cut the stratigraphy of the Hunstanton and Ferriby Formations in eastern England (Text-figs 3, 5). CL imagery of the calcite cement defines three zones (Text-fig. 8a). The earliest (Zone A) consists of small, non-luminescing crystals that have grown on the inside of the ventral valve. This is followed by Zone B, a wide expanse of brightly luminescing calcite, and then by Zone C with more modest luminescence. Staining (Text-fig. 8b) demonstrates the enrichment of ferroan calcite in Zone C. EMPA shows a well defined pattern of trace elements (Text-fig. 9).

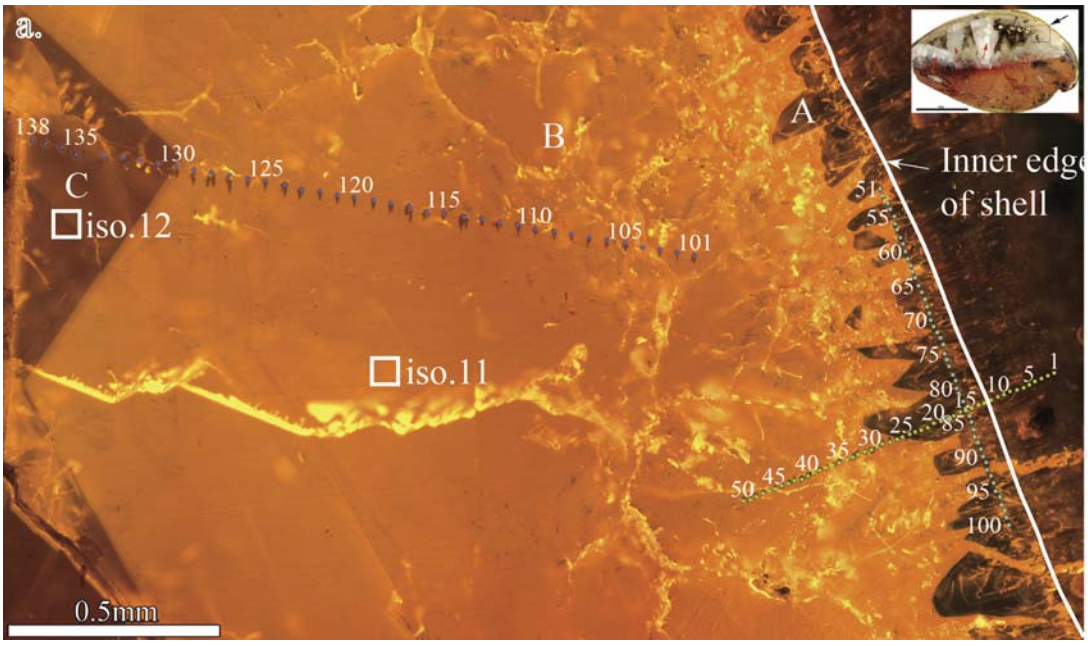

Text-fig. 8a. CL image of calcite cement in terebratulid brachiopod T1. Zone A consists of non-luminescent crystals attached to the inner wall of the ventral valve, Zone B is bright orange, Zone C is dull orange. The transects of EMPA (1-138) are clearly seen, the location of isotope analyses are shown

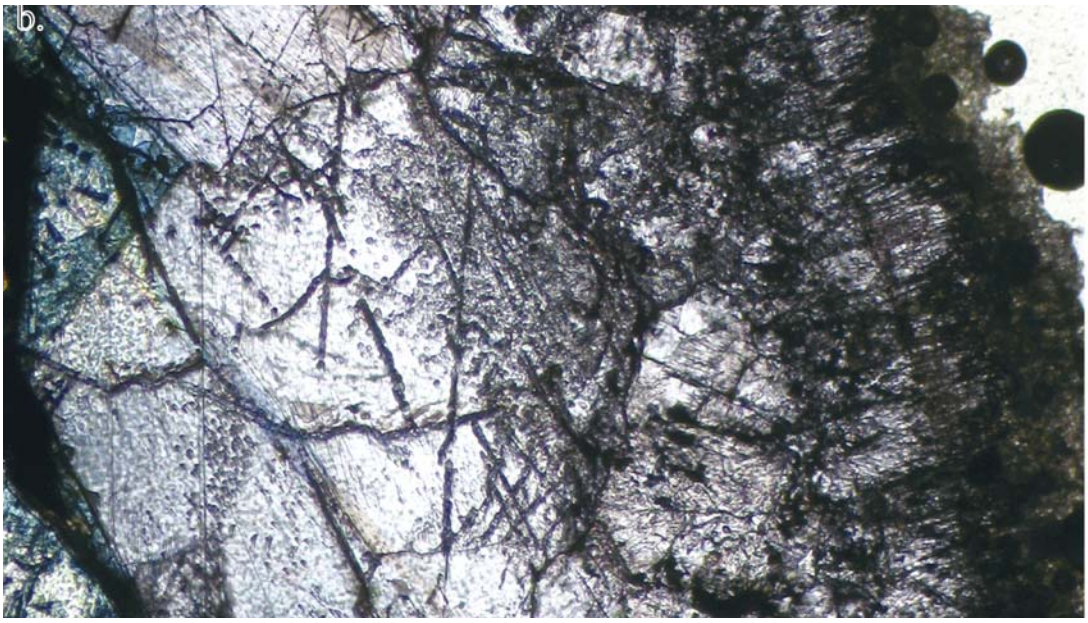

Text-fig. 8b. The same field of view as Text-fig. 8a but under PPL (plain polarized light) and stained. Zone B stains as non-ferroan calcite (pink), Zone C stains as ferroan calcite (blue)

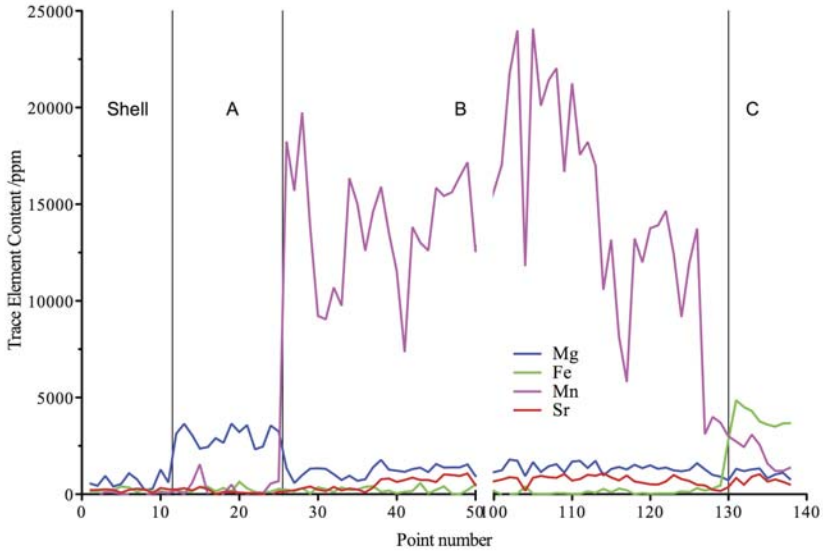

Text-fig. 9. Crossplot of trace element concentrations arranged along the direction of crystal growth for cement zones A, B and C and the shell of terebratulid brachiopod T1

Zone A is enriched in Mg, Zone B has exceptionally high values of Mn (up to 24,000 ppm), and Zone C is dominated by Fe. Stable isotope analysis from zones B and C show increasingly low values of $\delta^{18}O$ (–6.4‰ to –9.6‰) and high values of $\delta^{13}C$ (1.1‰ to 2.8‰) as cementation proceeded. The data are summarized in Table 1.

Sample No.	C.L. zones	aver. Mg/ppm	aver. Fe/ppm	aver. Mn/ppm	aver. Sr/ppm	Iso. No.	$\delta^{18}O_{VPDB}$/‰	$\delta^{13}C_{VPDB}$/‰
T1	Shell	686	228	56	235	–	–	–
	A	2939	241	929	160	–	–	–
	B	1280	234	14286	602	11	-6.41	1.13
	C	1105	3985	2027	728	12	-9.63	2.8

Table 1. Summary of trace element and stable isotope data for terebratulid brachiopod T1

Terebratulids T4a (*Concinnithyris microsubundata* Mitchell) and **T4b** (*Nerthebrochus nosetrapensis* Mitchell) are from just above the middle of the Belchford Member (Ferriby Formation) at Speeton (Text-fig. 4). Terebratulid T4a must have been buried in a near-vertical position with its umbo beneath. The original void occupied the anterior half of the shell cavity; the floor was of red chalk sediment and the roof was the anterior parts of the dorsal and ventral valves. The shell cavity of terebratulid T4b is nearly completely occupied by calcite cement except for a little red chalk in the umbo region, suggesting that the brachiopod was buried in a vertical position. CL imagery showed that both brachiopods displayed similar patterns of zonation. Three zones are present (Text-fig. 10), the earliest (Zone B) displays oscillatory zoning and bright orange luminescence. Zone C shows the same luminescence but lacks the oscillatory zoning. Luminescence in Zone D is duller and is weak in Zone E. The early non-luminescent cement (cf. Zone A of terebratulid T1) is absent. EMPA shows a complex pattern of trace elements (Text-fig. 11) consisting of two components each sim-

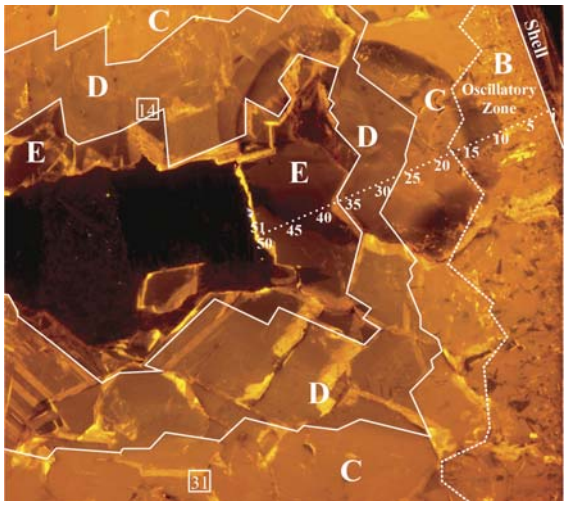

Text-fig. 10. CL image of the calcite cement in terebratulid brachiopod T4. Zones B, C and D are bright orange, Zone E is dull. The transect of EMPA (1–50) is clearly seen, the locations of stable isotope analyses 14 and 31 are indicatedacid insoluble residue (AIR) and the stable isotope values ($\delta^{18}O$, $\delta^{13}C$) of the calcite in the bulk sediment

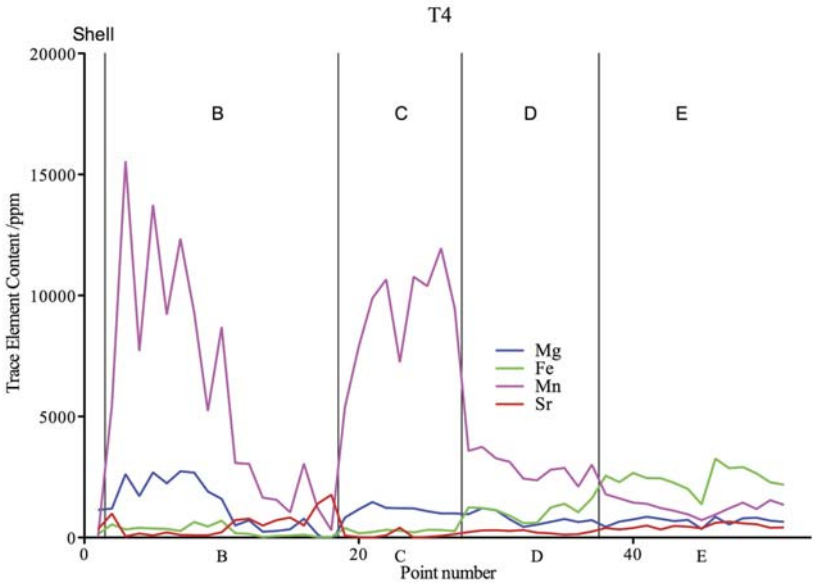

Text-fig. 11. Trace element concentrations arranged along the direction of crystal growth for the shell and CL zones B, C, D, and E in terebratulid brachiopod T4.

ilar to the first part of the pattern exhibited by terebratulid T1 (Text-figs 8, cf 10). Zone B has an earlier section with high Mn (up to 15,000 ppm) and high Mg (~2,500 ppm) and a later section with low Mn and Mg. Zone C repeats this pattern but at lower concentrations. Zones D and E show a gradual but marked increase in Fe until it is the dominant trace element. Four isotope analyses show that as cementation progressed there was a general decrease of $\delta^{18}O$ values from –4.7‰ to –8.7‰ and increasingly high values of $\delta^{13}C$ from 1.3‰ to 2.9‰. The data are summarized in Table 2.

Terebratulid T11 is from the Louth Member (Ferriby Formation) at Speeton (Text-fig. 4). The brachiopod was buried lying on its side and the void was located in the upper part of the shell cavity – its floor was chalk sediment and the roof was part of the dorsal and ventral valves. The void is now completely filled with calcite cement. Some of the cement crystals have been fractured and partly crushed, probably by compaction. CL imagery reveals three zones (Text-fig. 12a).

There is a trace of Zone A with its minute non-luminescing crystals on the inside of the valves. Zone B has very bright luminescence and Zone C is oscillatory in its early stages and is bright orange. EMPA reveals a complex chaotic pattern of trace elements (Text-fig. 13) with Sr particularly high in Zone B reaching values >3,000 ppm. There is an increase in Fe relative to Mn in Zone C and this is also indicated by staining (Text-fig. 12b). Stable isotope analyses from zones B and C show a progressive lowering of $\delta^{18}O$ from –7.2‰ to –7.6‰ and increasingly high $\delta^{13}C$ values from 2.8‰ to 3.5‰ as cementation progressed. The data are summarized in Table 3.

Terebratulid T12 (*Ornatothyris* sp.) is from the lower part of the Paradoxica Bed, Hunstanton (Text-fig. 6). The brachiopod was buried upside down with its dorsal valve below. The original void occupied the anterior part of the shell cavity. Its floor was chalk sediment and its roof was the anterior part of the ventral valve. The void is now filled by calcite cement. CL imagery reveals well

Sample No.	C.L. zones	aver. Mg/ppm	aver. Fe/ppm	aver. Mn/ppm	aver. Sr/ppm	Iso. No.	$\delta^{18}O_{VPDB}$/‰	$\delta^{13}C_{VPDB}$/‰
T4	Shell	1142	143	76	350			
	B	1303	279	6011	544			
	C	1132	278	9299	83	16	1.27	-4.71
						15	1.28	-4.81
						31	1.3	-5.26
	D	783	1102	2934	232	14	2.88	-8.67
	E	687	2445	1281	463			

Table 2. Summary of trace element and stable isotope data for terebratulid brachiopod T4

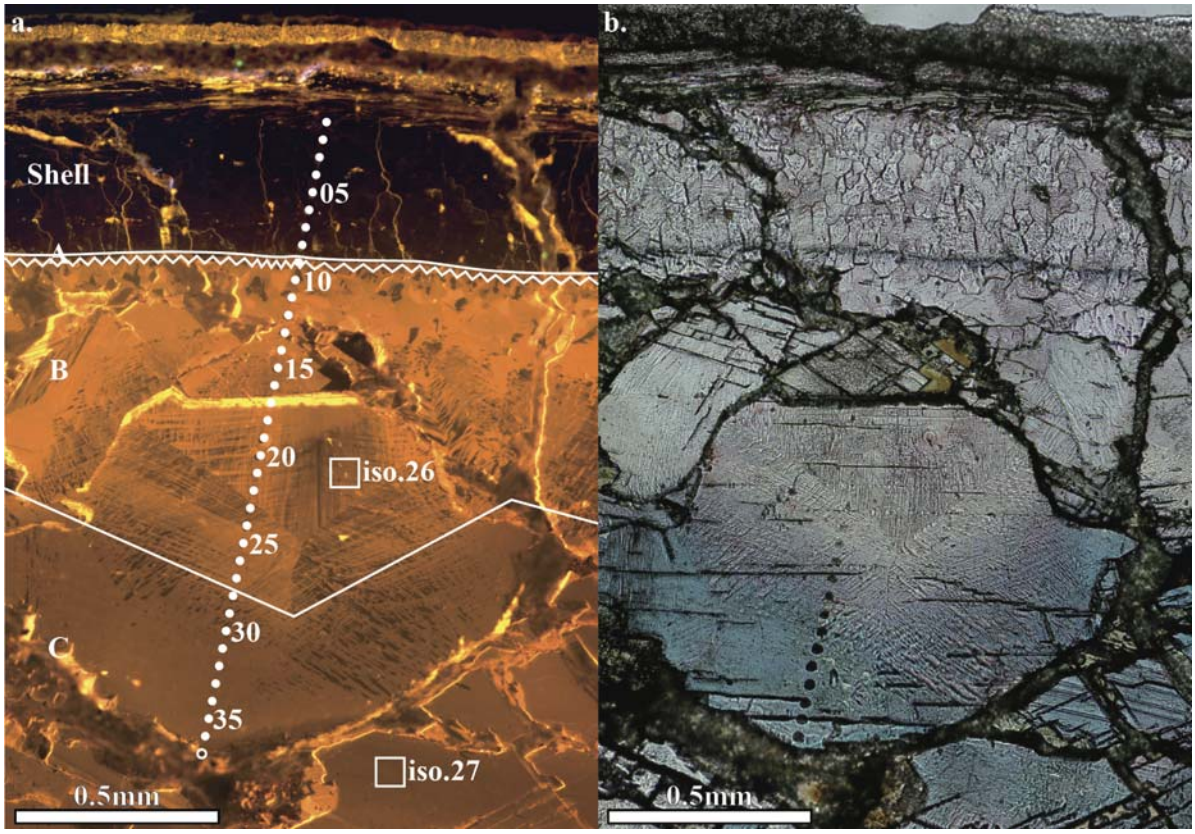

Text-fig. 12. a. CL image of the calcite cement in terebratulid brachiopod T11. Zone A with non-luminescing crystals line the interior surface of the shell. Zone B is bright orange, Zone C with oscillatory zoning is slightly duller. The transect for EMPA (1–37) is clearly seen. Location of stable isotope analyses (26, 27) are indicated b. The same field of view as Text-fig. 12A but under PPL and stained. Zone B is stained pink (non-ferroan calcite). Zone C is stained blue (ferroan calcite). Some of the calcite crystals show regions of crushing

developed growth zonation and the presence of six zones which are comparable to zones D to I in terebratulid T16

EMPA demonstrate (Text-fig. 14a) a pattern of trace elements (Text-fig. 15) matching very closely the pattern exhibited in terebratulid T16 and it is con-

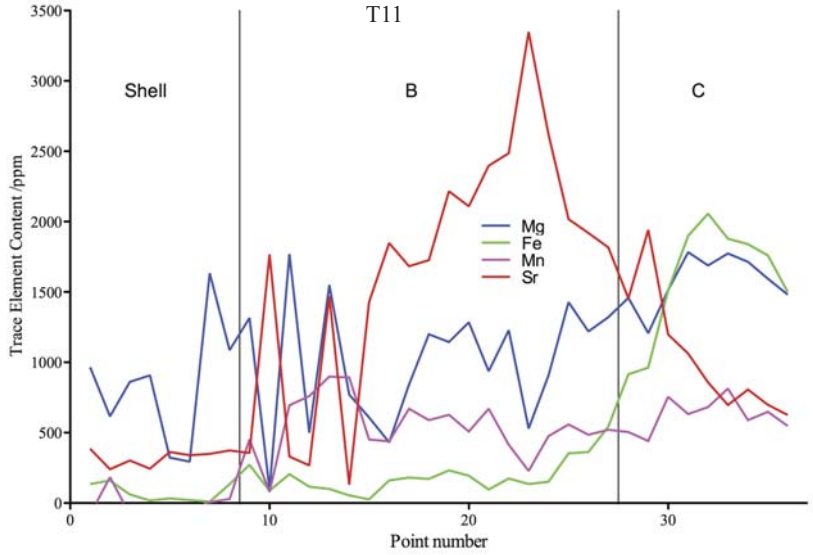

Text-fig. 13. Trace element concentrations arranged along the direction of crystal growth for zones B and C in terebratulid brachiopod T11

Sample No.	C.L. zones	aver. Mg/ppm	aver. Fe/ppm	aver. Mn/ppm	aver. Sr/ppm	Iso. No.	$\delta^{18}O_{VPDB}$/‰	$\delta^{13}C_{VPDB}$/‰
T11	Shell	71	-19	325	836			
	B	191	548	1681	1005	26	-7.15	2.82
	C	1592	624	1038	1580	27	-7.6	3.52

Table 3. Summary of trace element and stable isotope data for terebratulid brachiopod T11

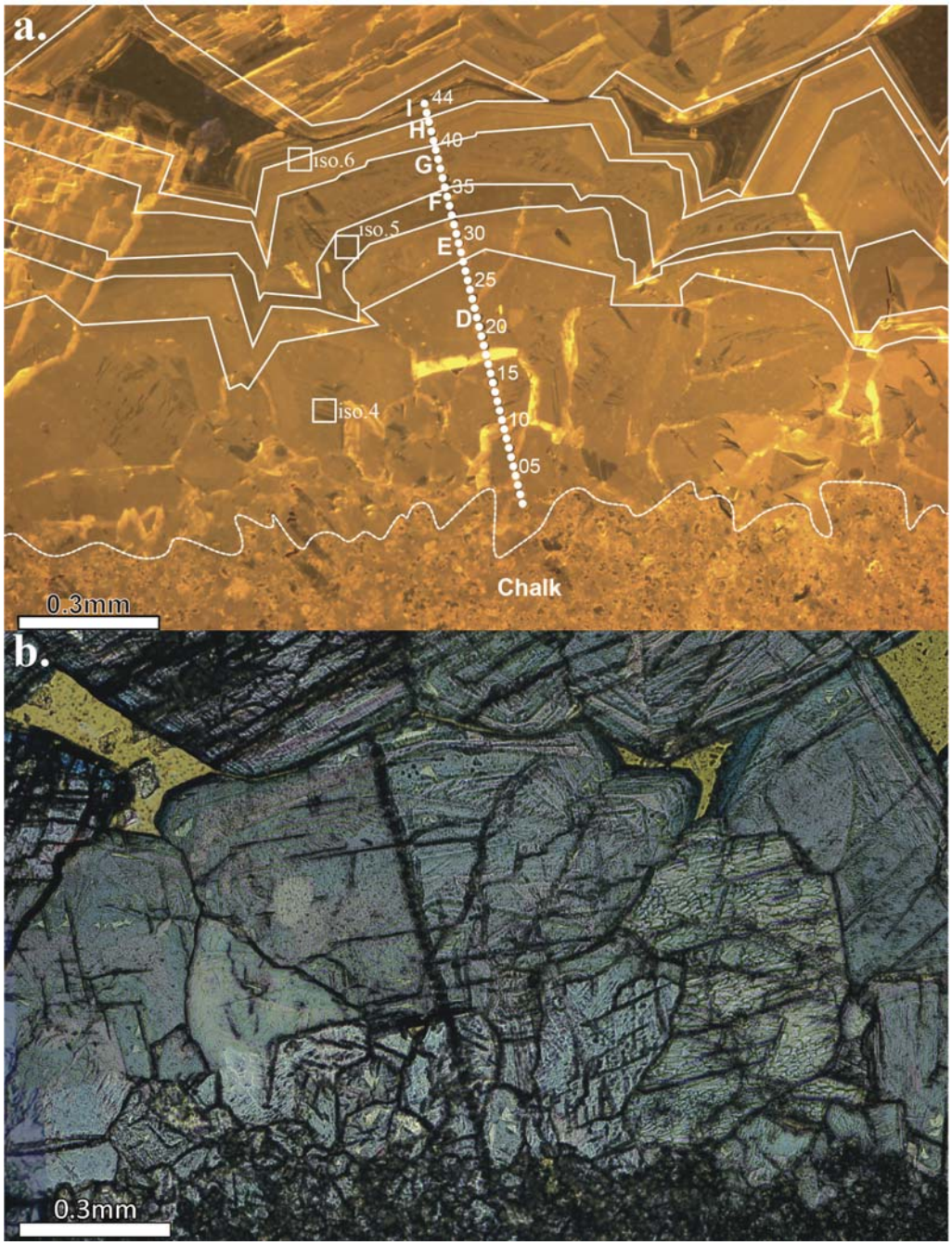

Text-fig. 14. a. CL image of the calcite cement with well developed growth zonation in the lower part of the vug in terebratulid brachiopod T12. Zones A, B and C present in terebratulid T16 are missing. Zones D to H show distinctive variations in their orange luminescence. Zone I is orangey-brown. The transect for EMPA (1–44) is clearly seen. Locations of stable isotope analyses (4, 5, 6) are indicated. b. The same field of view as 14A but under PPL and stained. Zones D to F are mauve and purple, zones H and I are blue (ferroan calcite)

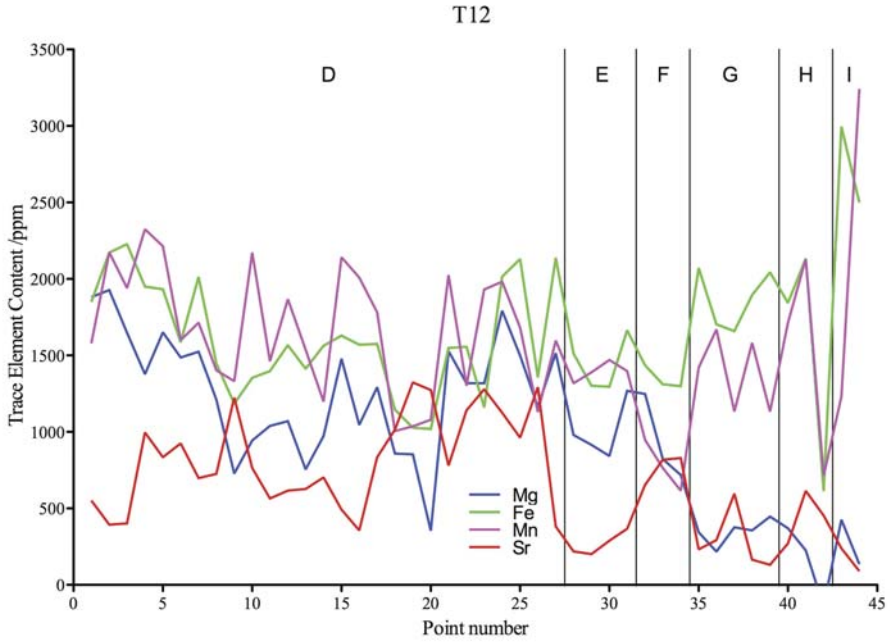

Text-fig. 15. Trace element concentrations arranged along the direction of crystal growth for cement zones D to I in terebratulid brachiopod T12

cluded that these are the same zones and have been given the same notation (D to I). Staining (Text-fig. 14b) demonstrates the enhanced Fe contents in the later cement zones. Stable isotope analyses from Zones D, F and H/I, shows a marked lowering of $\delta^{18}O$ values from –7.4‰ to –10.1‰ and $\delta^{13}C$ values from –1.4‰ to –5.6‰. The data are summarized in Table 4.

Terebratulid T16 (*Ornatothyris* sp.) is from the upper part of the Paradoxica Bed, Hunstanton (Text-fig. 6). The brachiopod was buried at a steep angle with its ventral valve uppermost (Text-fig. 7). The original void was at the anterior end of the shell cavity; its floor was of chalk sediment and its roof the anterior part of the dorsal valve. Cement now fills much of the void. CL imagery reveals strong growth zonation and eleven zones (A to K), are distinguished (Text-fig. 16). Corrosion surfaces define the outer margins of zones B, H and J. The earliest zones, A1 and A2, are well devel-

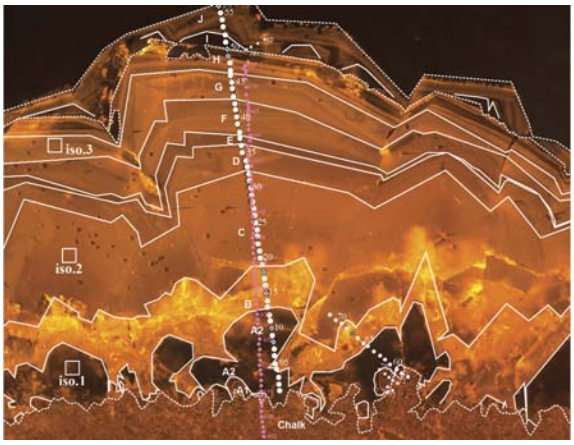

Text-fig. 16. CL image of the calcite cement with well defined growth zonation in the lower part of the vug in terebratulid brachiopod T16. The non-luminescent zone A is subdivided into an earlier phase A1 of very small crystals and a later phase A2 of larger crystals. Zone B is bright yellowish-orange. Zones C to H are orange displaying well marked variations in brightness. Zones I and J are dark orangey-brown. There are well marked corrosion surfaces between zones B and C, H and I, and I and J. Transects for EMPA are clearly seen. Locations of stable isotope analyses (1, 2, 3) are indicated

Sample No.	C.L. zones	aver. Mg/ppm	aver. Fe/ppm	aver. Mn/ppm	aver. Sr/ppm	Iso. No.	$\delta^{18}O_{VPDB}$/‰	$\delta^{13}C_{VPDB}$/‰
T12	D	1268	1612	1675	825	4	-7.44	-1.38
	E	1001	1444	1394	269			
	F	930	1349	776	767	5	-8.64	-2.72
	G	348	1874	1388	284			
	H	298	1988	1922	443	6	-10.14	-5.57
	I	281	2748	2236	165			

Table 4. Summary of trace element and stable isotope data for terebratulid brachiopod T12

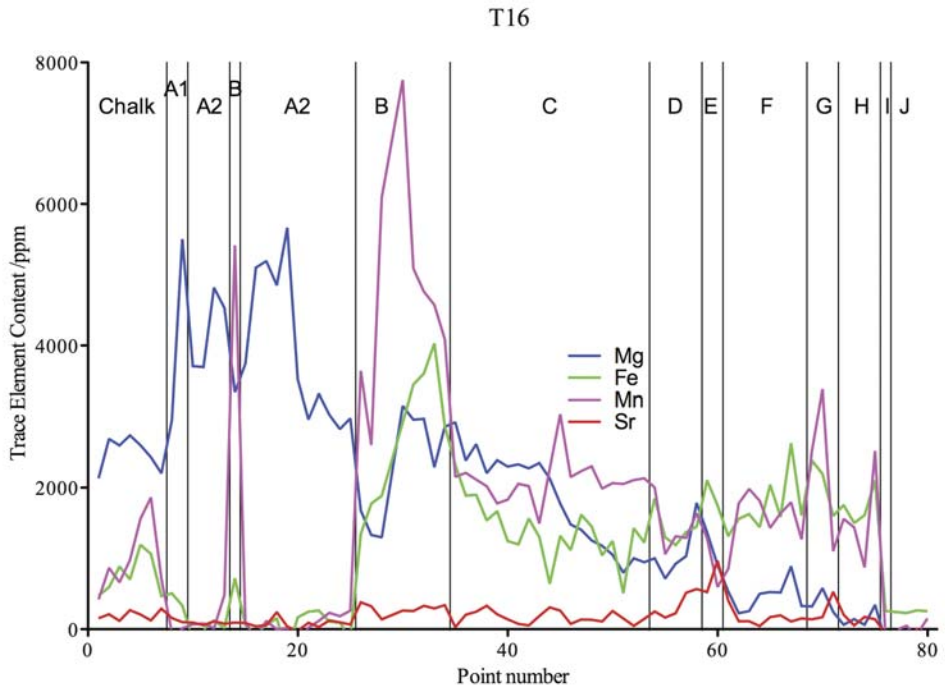

Note: the point data used here is renumbered according to the calcite growing direction, points 601 to 675 from analysis line 6 are renumbered as 1 to 75, then points 51 to 55 are renumbered as 76 to 80

Text-fig. 17. Crossplot of trace element concentrations arranged along the direction of crystal growth for the chalk and cement zones A to J in terebratulid brachiopod T16

oped on the floor of the void, consisting of dark non-luminescing calcite – these zones are absent from the cement growing from the roof. Zone C is brightly luminescent, whereas zones D to I display alternations of more or less dull orange luminescence. Zones J and K are dark, showing no luminescence. EMPA shows that there is a well defined change in trace element chemistry during cementation (Text-fig. 17). The non-luminescent zones A1 and A2 are rich in Mg (up to > 4,000 ppm) and low in Fe, Mn and Sr. In subsequent zones Mg drops gradually until it is undetectable in zones I and J. Strontium is low throughout, peaking at 750 ppm in Zone E. Manganese (~4,800 ppm) and Fe (up to 2,100 ppm) are enriched in zones B and C; these two trace elements dominate zones D to H. Zones I and J have very low trace element content. Text-fig. 17 shows how the later cement zones (D to H) become increasingly enriched in ferroan calcite. Stable isotope analyses from zones A–B, C–D and G–H–I–J show that $\delta^{18}O$ values decrease from –5.3‰ to –8.3‰ and $\delta^{13}C$ values from –1.5‰ to –5.8‰. The data are summarized in Table 5.

Sample No.	C.L. zones	aver. Mg/ppm	aver. Fe/ppm	aver. Mn/ppm	aver. Sr/ppm	Iso. No.	$\delta^{18}O_{VPDB}$/‰	$\delta^{13}C_{VPDB}$/‰
T16	Chalk	2485	769	1009	197			
	A1	4228	421	0	130	1	-5.33	0.58
	A2	4099	0	146	86			
	B	2319	2735	4825	291			
	C	1831	1381	2106	164	2	-8.17	-1.46
	D	1092	1432	1462	345			
	E	1138	1929	942	748			
	F	472	1727	1570	163			
	G	382	2059	2338	280	3	-8.3	-5.84
	H	153	1743	1598	144			
	I	0	258	0	0			
	J	0	250	39	0			

Table 5. Summary of trace element and stable isotope data for terebratulid brachiopod T16

Terebratulids T2, T3, T5 to T10, T13 toT15. For each of these brachiopods the CL imagery of the cement and the point locations of the EMPA are shown in Text-fig. 18. EMPA demonstrates that the trace element patterns in these vugs (Text-Fig. 19) are very variable, displaying little resemblance to the well-ordered patterns in terebrat-

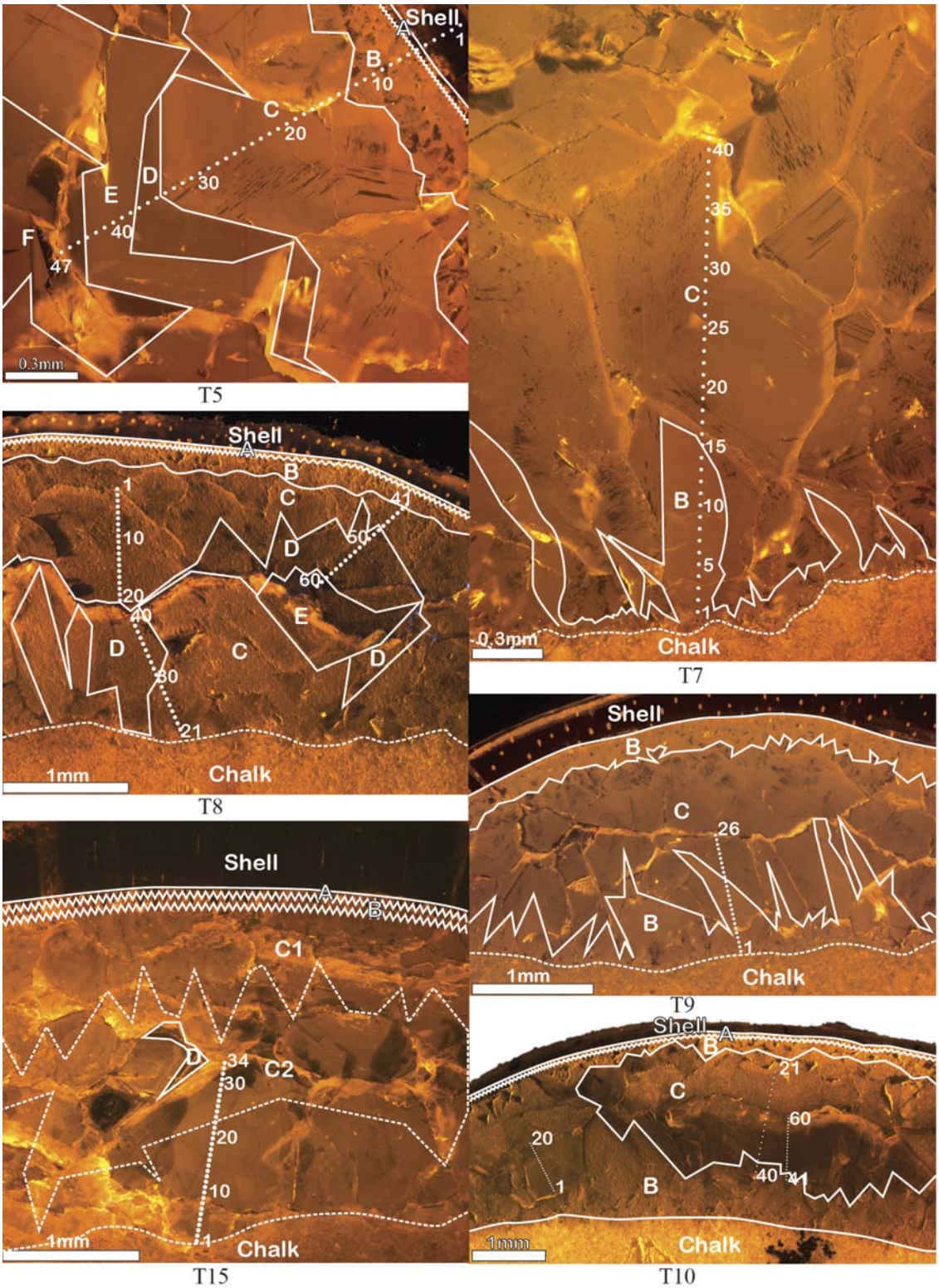

Text-fig. 18. CL image of the calcite cement and EMPA transects for terebratulid brachiopods T2, T3, T5–T10, T13–T15.

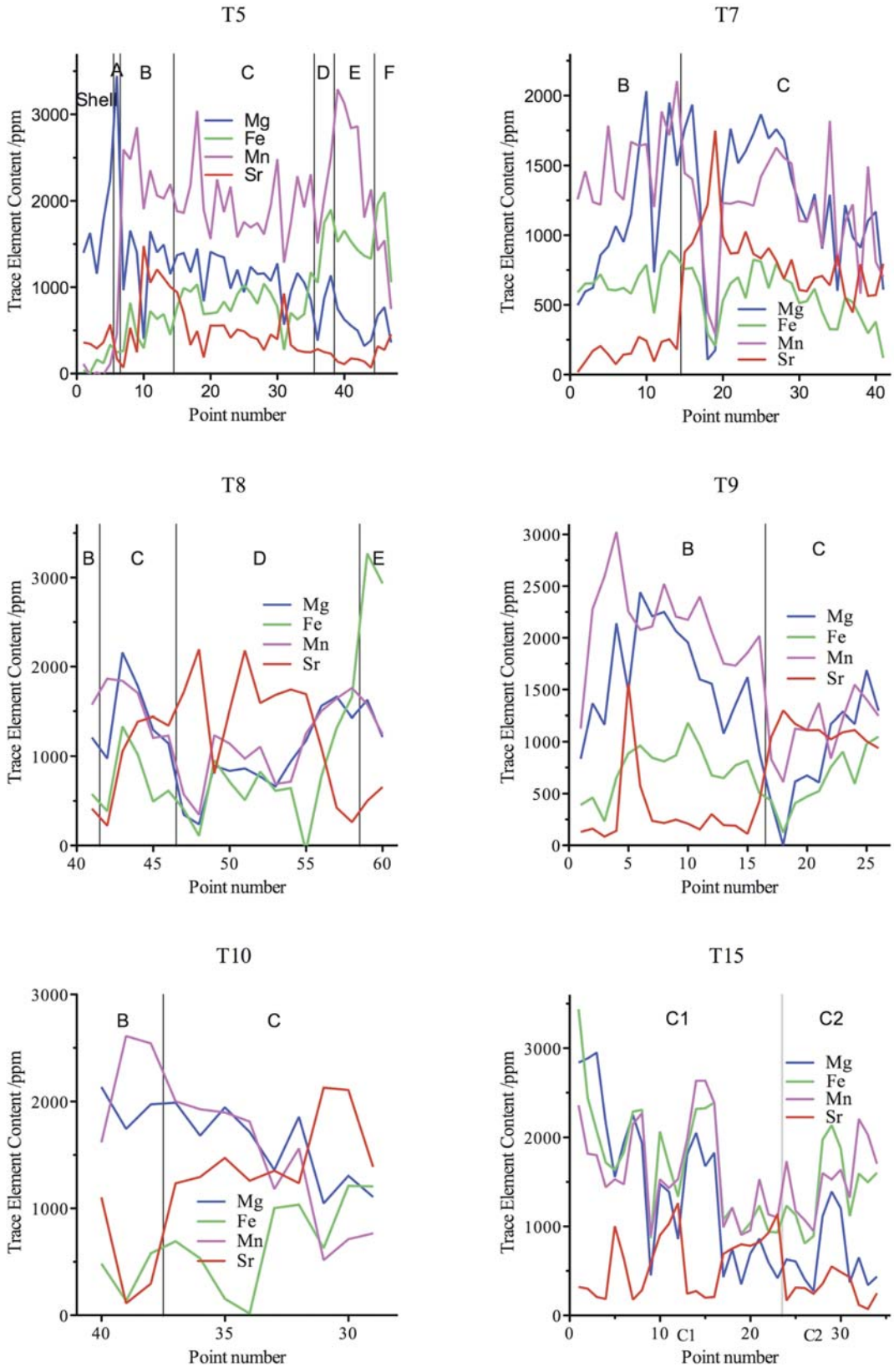

Text-fig. 19. Crossplot of trace element concentrations arranged along the direction of crystal growth for the chalk and cement zones in the brachiopods imaged in Text-fig. 18

Sample	Zone	Mg/ppm	Fe/ppm	Mn/ ppm	Sr/ppm	Iso. No.	$\delta^{18}O‰$	$\delta^{13}C‰$
T15	C1	1486	1739	1640	598			
	C2	676	1443	1542	301	10	-8.29	-2.72
T10	B	1453	587	1584	1170	24	-5.61	1.46
	C	1655	1382	1376	1370	25	-7.33	2.40
T9	B	1626	730	2137	309	34	-6.11	1.72
	C	892	625	1131	1092	23	-11.55	-0.47
T8	B	577	1211	1574	415	—	—	—
	C	746	1379	1442	1157	21	-7.36	2.26
	D	787	1241	1312	1240	22	-8.05	2.63
	E	3104	1421	1411	579	20	-8.54	2.83
T7	B	1132	678	1529	163	33	-7.18	2.14
	C	1258	538	1160	829	19	-7.93	2.13
T5	shell	1641	0	48	386	—	—	—
	A	3447	246	457	172	—	—	—
	B	1266	539	2310	837	—	—	—
	C	1142	824	1957	463	32	-6.45	2.13
	D	798	1566	2014	255	—	—	—
	E	523	1474	2678	133	—	—	—
	F	600	1708	1238	350	17	-8.25	2.18
T14	C	—	—	—	—	7	-7.49	-0.37
	C	—	—	—	—	8	-9.63	-6.59
T13	C	—	—	—	—	9	-8.29	-2.81
T6	C	—	—	—	—	18	-7.94	2.09
T3	C+	—	—	—	—	28	-8.17	2.23
T2	C	—	—	—	—	30	-6.66	1.18
	D	—	—	—	—	29	-7.85	2.45

Table 6. Summary of trace element and stable isotope data for terebratulid brachiopods T2, T3, T5 toT10, T13 toT15

ulids T1, T4, T12 and T16. The average trace element values for each CL zone and the $\delta^{18}O$ and $\delta^{13}C$ values are listed in Table 6. Terebratulids T2, T7 and T8 are *Atactosia jeansi* Mitchell; T3 and T5 are *Nerthebrochus nosetrapensis* Mitchell; T6 is *Concinnithyris microsubundata* Mitchell; T13 is *Concinnithyris subundata* (J. de C. Sowerby); and T14 and T16 are *Ornatothyris* spp.

COMPARISON OF CEMENTS FROM SPEETON AND HUNSTANTON

Text-figs 20 and 21 show the average trace element concentration and available stable isotope values for each cathodoluminescent zone in the cement in brachiopods T1 and T12–16 which respectively represent the cementation at Speeton and Hunstanton. Differences are marked. Growth zones are rare or absent in T1 whereas they are frequent in T12–16 (Text-figs 8a, 16). Corrosion surfaces are present in T12–16; they are absent in T1. Both T1 and T12–16 display an earliest phase of cement which is non-luminescent, enriched in Mg (up to 4,000 ppm) and empoverished in Fe, Mn and Sr. In T1 this is followed by a wide zone of exceptionally high Mn content (up to 24,000 ppm), whereas in T12–16 this zone shows alternating enrichment in Mn and Fe as the overall trace element concentration decreases with these two elements becoming co-dominant in the latest cement stages. In contrast, the high Mn zone of T1 is replaced at much lower concentrations by a zone dominated by Fe (up to 4,000 ppm). Detailed comparison between the trace element patterns are hindered because there are no marker points to tie the two sequences together. We consider that (a) the earliest non-luminescent Mg-rich cements in the Speeton and Hunstanton brachiopods are equivalents; and (b) the overall differences in patterns are significant and do not reflect just the absence of a continuous and complete cementation history. Evidence in support of this difference in cementation history comes from the stable isotope record, however incomplete it may be. In brachiopod T1 isotope analyses 11 and 12 from respectively CL zones

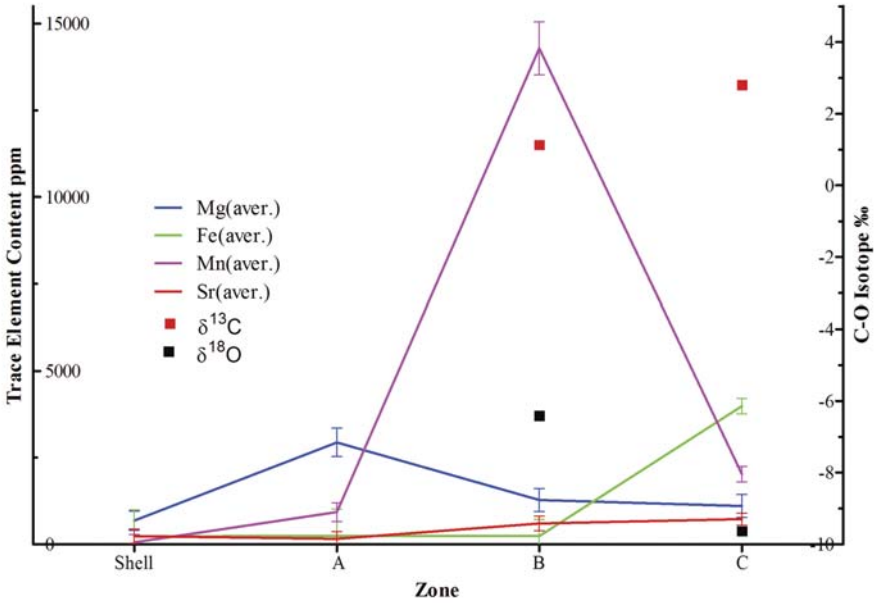

Text-fig. 20. Average trace element values and isotope values arranged along the direction of crystal growth for the typical example (terebratulid brachiopod T1) of suboxic cementation from Speeton

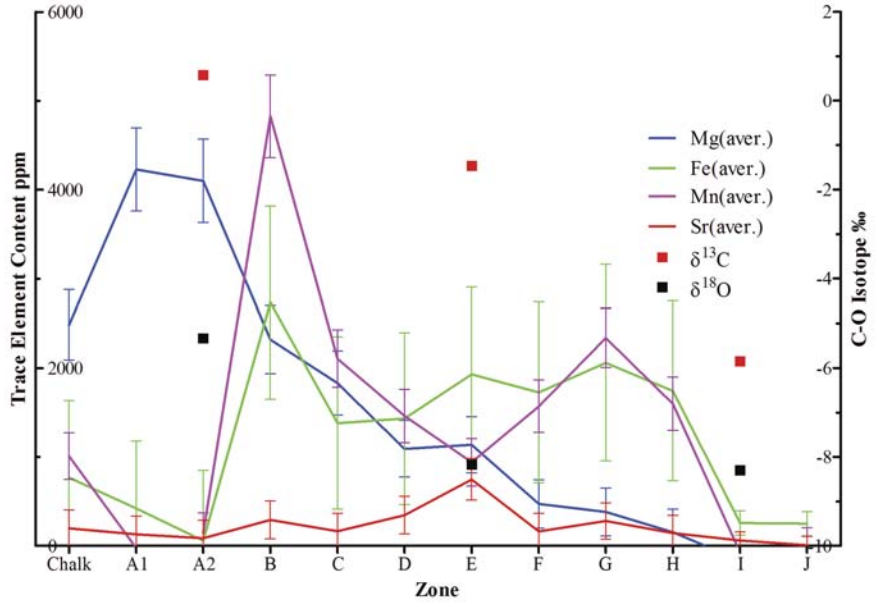

Text-fig. 21 Average trace element values and isotope values arranged along the direction of crystal growth for the typical example (combined terebratulid brachiopods T12–16) of anoxic cementation from Hunstanton

B and C display a distinct lowering of $\delta^{18}O$ from –6.4‰ to –9.6‰ and increasingly high $\delta^{13}C$ values from 1.1‰ to 2.8‰. The isotope data in T12–16 from the earliest cement (Zone A) have a $\delta^{18}O$ value of –5.3‰ and a $\delta^{13}C$ of 0.6‰. Analyses of later cements display a general lowering, with very minor oscillation of $\delta^{18}O$ and $\delta^{13}C$ values: Zone C, $\delta^{18}O$ –8.2‰, $\delta^{13}C$ –1.5‰; Zone D, $\delta^{18}O$ –7.4‰, $\delta^{13}C$ –1.4‰; Zone F, $\delta^{18}O$ –8.6‰, $\delta^{13}C$ –2.7‰; Zone G, $\delta^{18}O$ –8.3‰, $\delta^{13}C$ –5.8‰; Zones H/I, $\delta^{18}O$ –10.1‰, $\delta^{13}C$ –5.6‰.

These same two patterns of cement evolution are seen when all the stable isotope data from the 18 brachiopods are considered. Text-fig. 22 shows how the Speeton brachiopods are confined to the positive $\delta^{13}C$ area of the crossplot, whereas the Hunstanton brachiopods are restricted to the negative $\delta^{13}C$ area. In

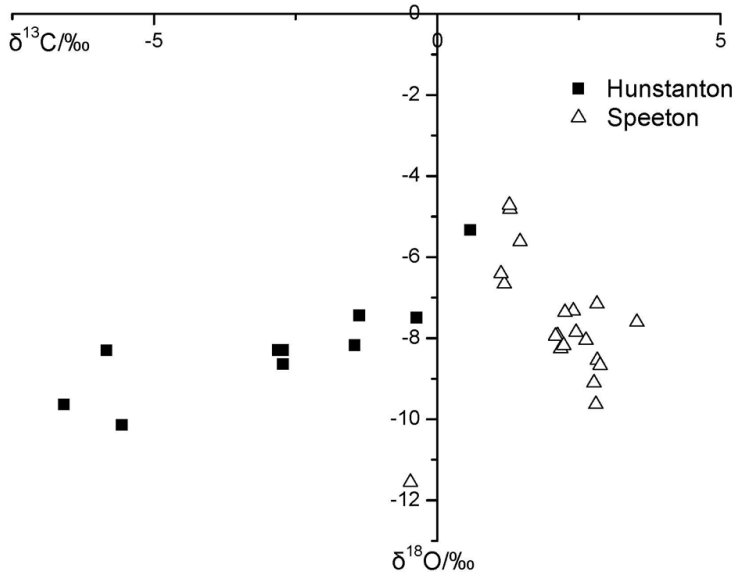

Text-fig. 22. Crossplots of all $\delta^{18}O$ and $\delta^{13}C$ analyses from the cement filled vugs in the terebratulid brachiopods from Speeton and Hunstanton

each group there is a single exceptional value, The exception from Hunstanton is T12–16 isotope analysis 1 of the earliest cement (non-luminescent Mg-rich) which has a positive $\delta^{13}C$ value. This is the only isotope analysis from this cement from either group – it is typically so thin that uncontaminated samples are unattainable – we assume that this cement in both groups has a positive $\delta^{13}C$ value. The exception from Speeton, isotope analysis 23, is of the late cement in brachiopod T9 from the Grey Bed. This bed has a lithology resembling the Paradoxica Bed in the presence of glauconite but lacking its hardground development; it is sandwiched between units of pink and red chalk at the base of the Candlesby Member and the top of the Bigby Member of the Ferriby Formation (Text-fig. 4). The earlier of the two analyses from this brachiopod has a $\delta^{13}C$ value of 1.7‰ but the later cement is –0.5‰.

The range of $\delta^{18}O$ displayed by both the Speeton and Hunstanton brachiopods is broadly similar, between –4‰ and –11‰. Text-fig. 23 shows that the values from the brachiopods at the two locations are evenly distributed in this range.

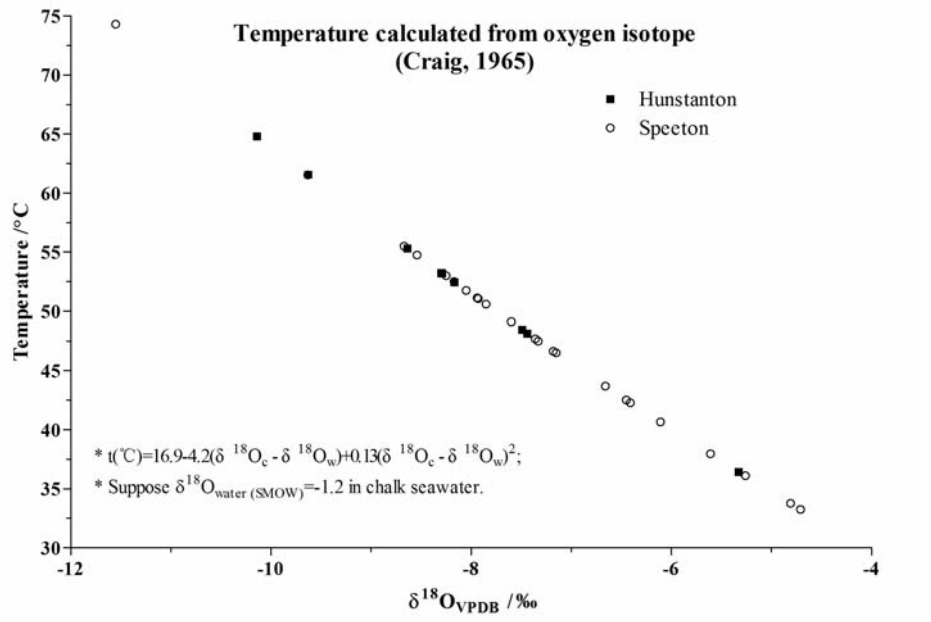

Text-fig. 23. Crossplot of $\delta^{18}O$ values and temperature (based on Craig 1965) for calcite cements from terebratulid brachiopods from Speeton and Hunstanton

GENERAL SETTING OF THE CENOMANIAN CHALKS AT SPEETON AND HUNSTANTON

The sedimentological habitat in which the brachiopods lived at Speeton and Hunstanton were quite different. They were approximately 140 km apart, both were fully marine. Speeton is characterized by pink and red chalks deposited nearly continuously at the margin of the North Sea Basin. Pauses in sedimentation were never long enough for hardgrounds to develop. Early lithification was restricted to local patches of cementation associated with the decomposition of the soft parts of large ammonites or the development of nodules (Jeans 1980). Compaction and the movement of porefluid in the unlithified parts of the chalk were extensive. Hunstanton was on the shallow margin of the East Midland Shelf. The

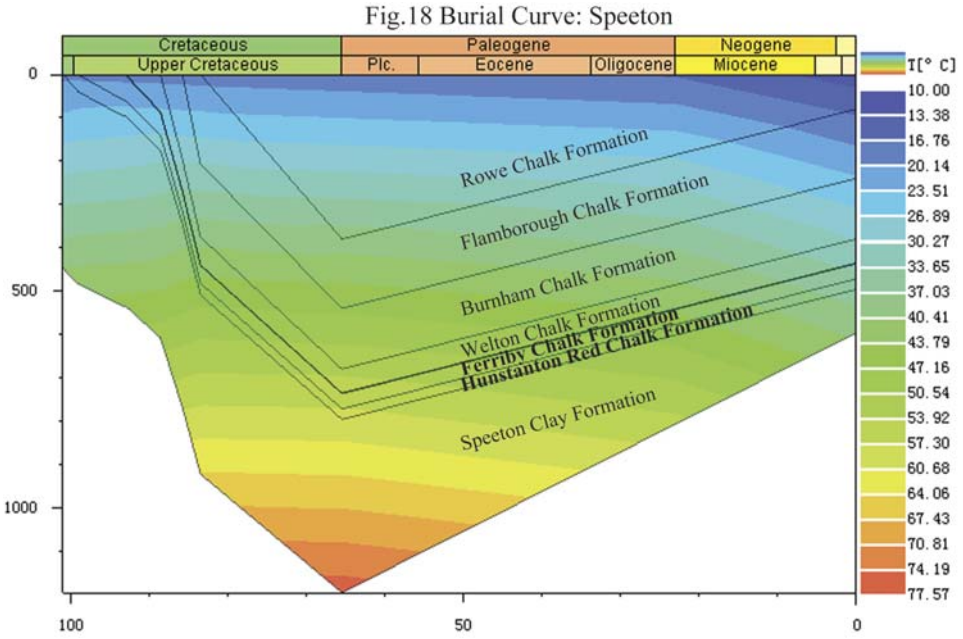

Text-fig. 24. Burial and palaeotemperature curve for the Ferriby and Red Chalk formations at Speeton, Yorkshire

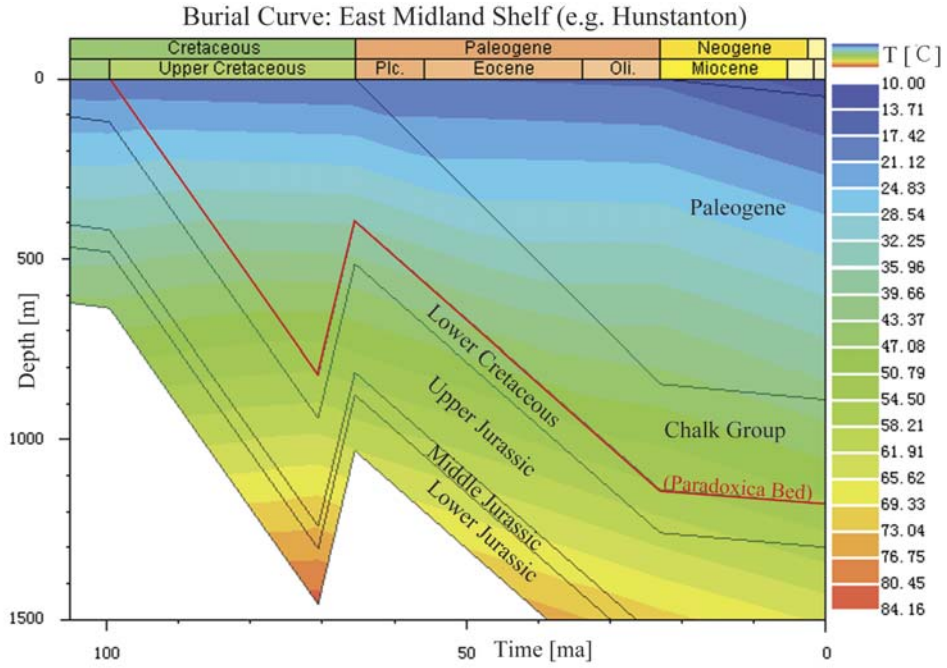

Text-fig. 25. Burial and palaeotemperature curve for the Paradoxica Bed hardground at the base of the Ferriby Formation at Hunstanton, Norfolk

sediments were coarser grained and periods of non-deposition restricted their accumulation. The extensive development of the Paradoxica Bed hardground at the expense of pink and red coloured chalk over much of the East Midland Shelf was a major feature. To what extent the subsequent geological history of these contrasted areas influenced the cementation history recorded in the shell cavities of their brachiopods is an important consideration. For example, Speeton is located within the Howardian-Flamborough Fault Zone which was active from Jurassic to Tertiary times. It is responsible for the spectacular contortion zones in the Chalk near to Speeton (e.g. Phillips, 1829, Lamplugh 1895; Starmer 1995). These zones are associated with extensive pressure dissolution of the Chalk. Hunstanton is on the edge of the East Midland Shelf close to the hinge line (Wash Line of Jeans 1980) which marks its southern structural edge. Calculated burial depth curves for Speeton and Hunstanton are different (Text-figs 24, 25) but maximum estimated temperatures are similar (55–60°C).

INTERPRETATION

Significance of $\delta^{18}O$ values

The range of $\delta^{18}O$ values for the cements in the brachiopods from Speeton and Hunstanton are similar (Text-fig. 23), suggesting a similar pore water and temperature history. There is no doubt from the presence of fully marine fossil assemblages that the original pore waters of the chalk sediment were fully marine at both locations. The general trend in the cement from individual brachiopods is from less to more negative values (Tables 1–6). In brachiopods T12–16 from Hunstanton there are minor fluctuations in $\delta^{18}O$ values (Text-fig. 21) which may be related to the influx of cooler marine pore water of varying oxygen isotope values; variations in the oxygen contents of these waters could be responsible for the antipathetic relationship between Fe and Mn in the calcite cement of zones C to F. However the general trend to more negative values is maintained as cementation progressed.

The palaeotemperature-burial curves (Text-figs 24, 25) for the Cenomanian Chalk at Speeton and Hunstanton suggest similar maximum temperatures of 55–60°C, somewhat less than the maximum temperature of about 75°C predicted by the $\delta^{18}O/T°C$ plot shown in Text-fig. 23. Considering the uncertainties in constructing the burial curves in eastern England (Holliday 1999), and the possible influence of pore waters with $\delta^{18}O$ values other than that of Cretaceous seawater, it is suggested that calcite cementation in the brachiopod vugs at Speeton and Hunstanton took place probably in pore waters of marine origin over a temperature range of approximately 30 to 75°C.

Brachiopod and regional calcite cements

Important for interpreting the varying geochemistry of the cement in the vugs is its relationship to the bulk geochemistry of the different types of lithification of the chalk caused by calcite cementation at various times during diagenesis. In eastern England five types of early lithification preceded the late regional cementation, all with a characteristic relationship between the Fe geochemistry and calcite precipitation (Jeans 1980).

At Speeton two types of early lithification pre-date the regional cementation. Both display a pattern of Fe geochemistry in which $Fe(OH)_3$ (assumed precursor of the red hematite pigment) has been dissolved in association with the precipitation of an Fe-enriched calcite cement without the precipitation of Fe sulphides. Type-4 lithification occurs in the chalk infilling and adjacent to large ammonites. Type-5 occurs in the nodules of nodular chalks and marls. New trace element analyses show that these two types can be differentiated (Hu, Long and Jeans in press). The bulk calcite of Type-4 is enhanced in Mg, Mn and Fe relative to the surrounding matrix, whereas Type-5 is enhanced only in Fe relative to the matrix. This suggests that the cementation of the large ammonite and its surrounding chalk spanned the Mg-, Mn- and Fe-enriched phases recorded in the suboxic cement series of brachiopod T1 (Text-fig. 20), whereas the cementation of the nodules started much later spanning only the Fe-rich phase.

At Speeton there is considerable evidence of differential compaction in the chalk which had not been affected by early lithification (Jeans 1980). This must have involved the movement of fluids of varying chemistry reflecting different stages in the evolution of the pore water and is thought responsible for the irregular trace element patterns in many of the Speeton brachiopods (Text-fig. 26). Where early lithification had occurred the pore fluid-sediment system was stabilized and isolated from the compaction driven pore fluids of variable chemistry. This allowed the distinctive trace element patterns seen in brachiopod T1 to develop.

New isotope data from the Louth Member (Ferriby Formation) at Speeton (Hu, Long and Jeans in press) demonstrates that the late calcite cement associated with the regional hardening of the Chalk of eastern England is characterized by increasingly low $\delta^{13}C$ values, the reverse of the trend characteristic of suboxic cementation. The only example of such a reversal is associated with brachiopod T9 from the Middle

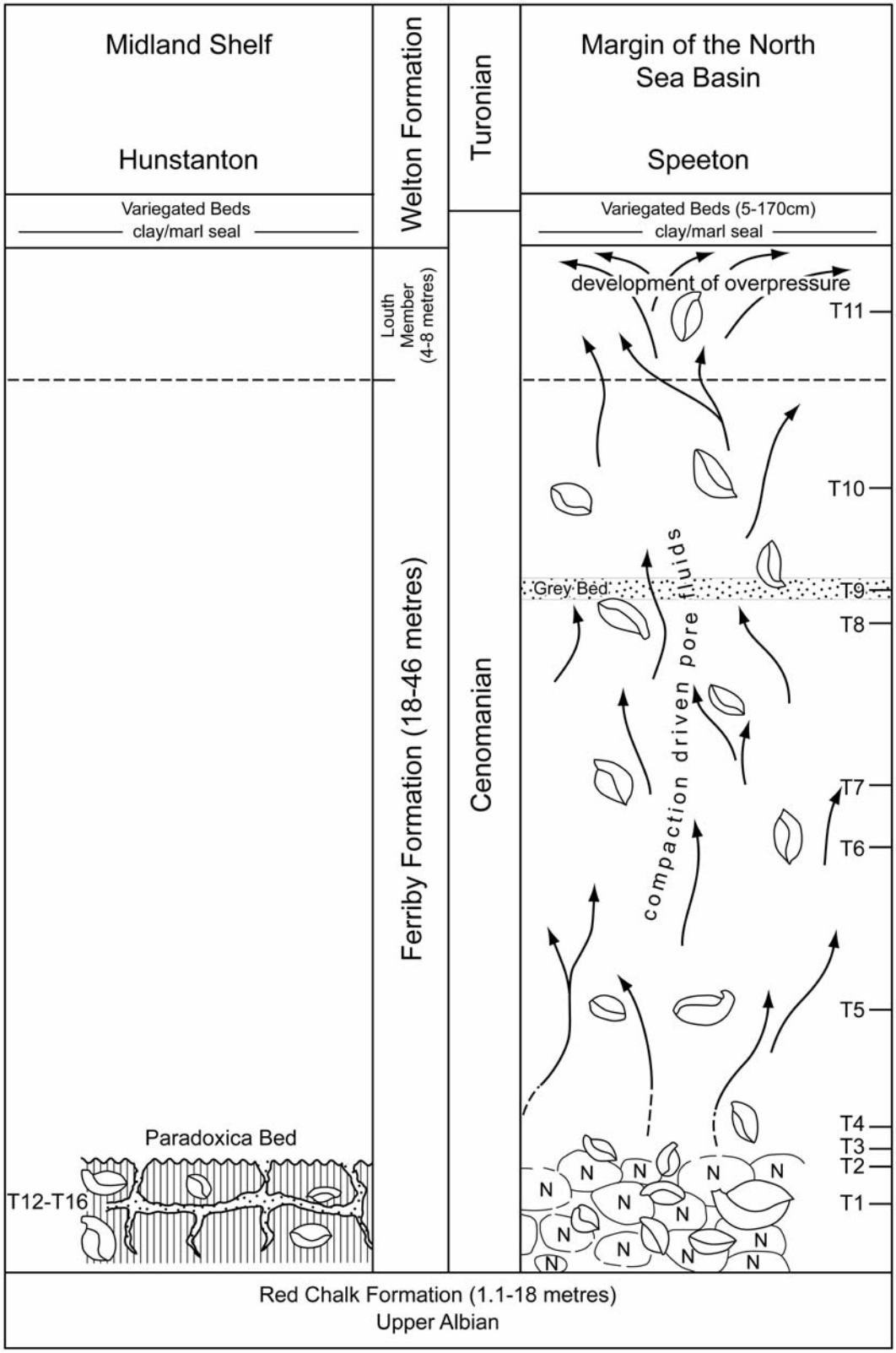

Text-fig. 26. A schematic interpretation of the diagenetic setting at Speeton and Hunstanton during the later stages of diagenesis prior to the lost porefluid pressure and to initiation of pressure dissolution-related calcite cementation. It shows the relationship between the development of overpressure by the effect of compaction-driven porefluids being trapped by clay-rich Variegated Beds (Plenus Marls) and the geochemical patterns recorded in the calcite cements within terebratulid brachiopods

Cenomanian Grey Bed, where it is related to the transition from suboxic to anoxic cementation. On present evidence the calcite responsible for regional cementation is not represented in any of the vugs from the Speeton brachiopods.

At Hunstanton the brachiopods come from the Paradoxica Bed hardground, an example of type-1 lithification (Jeans 1980). This lithification is of regional extent and is related to a surface of non-deposition; the underlying chalk has been stripped of its $Fe(OH)_3$ (assumed to be the precursor of the red hematite pigment) and lithified. The geochemistry of its bulk chalk shows an increasing Mg content towards the top surface of the bed. This suggests that the initial lithification of the Paradoxica Bed resulted from the precipitation of the early Mg-rich non-luminescent cement that is well developed in brachiopod T16 (Text-figs 16, 17).

$\delta^{13}C$ and trace element patterns

The initial evidence (Jeans 1980) for microbial control of early lithification in the Cenomanian Chalk of eastern England was its association with what must have been the rotting remains of large ammonites buried in coloured chalk with the partial dissolution of the original $Fe(OH)_3$ pigment in the sediment with the precipitation of an Fe-enriched calcite cement. This association between $Fe(OH)_3$ dissolution and Fe-enriched cementation was also evident in the development of (1) nodular chalks and marls; and (2) the Paradoxica Bed hardground at the top of and at the expense of red chalks (Belchford Member, Text-fig. 2) over much of the East Midland Shelf. There is the suggestion that hardground formation with its glauconite staining was restricted to chalk sediment where there had been a complete loss of $Fe(OH)_3$, as if the cements responsible for this type of lithification only became available once the last of the $Fe(OH)_3$ had been dissolved. The $\delta^{13}C$ and trace element patterns from the brachiopod vugs provide additional evidence of the geological constraints under which these early cements developed. The relationship between the two cement series demonstrates that within the time frame of diagenesis the suboxic series preceded the anoxic. At Hunstanton the very earliest cement in brachiopod T16 still has a positive $\delta^{13}C$ value before switching to negative values in subsequent phases of cements. At Speeton in brachiopod T9 from the Grey Bed this switch-over takes place at a much later stage of the cement sequence. The change from positive to negative $\delta^{13}C$ values may also be part of lateral changes in lithofacies. Brachiopods T1 (Speeton) and T12/T16 (Hunstanton) are from the same ammonite subzone (*Neostlingoceras carcitanense* Subzone) at the base of the Cenomanian: continuous sedimentation at Speeton has resulted in the suboxic cement series whereas at Hunstanton hardground development is dominated by the anoxic series. The geological setting of brachiopods T1 and T12–16 and the $\delta^{13}C$ and trace element patterns suggest that the cement series are parts of an overall pattern of early lithification.

Text-fig. 27 summarises this and related factors as well as our interpretation. The earliest cement (non-luminescent) is Mg-rich, with a low content of Fe and Mn, suggesting that the porewaters were oxic. The source of the Mg is likely to have been the dissolution of bioclasts of high Mg-calcite. The inferred occurrence of this cement in the ammonite chalk suggests that aerobic ammonification may have contributed to its precipitation (Jeans 1980, p. 140). The Mg-rich calcite cement is common to both cement series, whereas the two zones of suboxic cementation are restricted to the suboxic series. This is not considered a fundamental difference but may be related either to unsuitable conditions for cement precipitation or the rapid development of anoxia in the sediment which did not allow suboxic zones of cementation to develop. The cement of the first suboxic zone is Mn-rich but low in Fe, whereas the second is Fe-rich. This is interpreted as reflecting the sequential reduction of $Mn(OH)_4$ and $Fe(OH)_3$ in relation to their oxidation potential. Likely to have been responsible for this are anaerobic Mn- and Fe-reducing bacteria (e.g. *Geobacter*, *Pseudomonas*, *Desulfovibrio*) which oxidize a wide range of organic compounds with the production of HCO_3^- and H^- (Plante 2007). Examples of these reactions with acetate and formate substrates are shown below:

$$acetate^- + 8Mn^{4+} + 4H_2O \rightarrow 2HCO_3^- + 8Mn^{2+} + H^+$$
$$acetate^- + 8Fe^{3+} + 4H_2O \rightarrow 2HCO_3^- + 8Fe^{2+} + 9H^+$$
$$formate^- + 8Mn^{4+} + H_2O \rightarrow HCO_3^- + 2Mn^{2+} + H^+$$
$$formate^- + 8Fe^{3+} + H_2O \rightarrow HCO_3^- + 2Fe^{2+} + 2H^+$$

The production of hydrogen ions (H^+) would have resulted in the dissolution of calcite in the sediment providing an additional source of Ca^{2+} to that already present in the porewaters from the dissolution of high Mg-calcite and aragonite. The cements of the anoxic zone are dominated by Fe and Fe/Mn. Unlike the suboxic zones, where the source of the Mn and Fe is thought to be the hydroxide colouring pigment in the sediment, in the anoxic zone it is likely to be coarser-grained Fe and Mn-rich material that survived the restricted activities of the Mn- and Fe-reducing bacteria, but not those of the anaerobic sulphate-reducers which are capable of mobilizing this more resistant material. The sulphate-reducing bacteria utilise organic matter in the reduction of

sulphate anions with the production of H_2S and carbonate ions. With a ready source of Ca^{2+} ions calcite cement will precipitate. In sediments with a high iron and manganese content sulphides will form. If their content is low, as seems to have been the situation in the Paradoxica Bed, much of the H_2S may escape as gas bubbles or, if bioturbation has caused the invagination of oxic conditions, be oxidised as sulphurous or sulphuric acids which dissolve and etch the calcareous grains. Evidence of this is well known in modern carbonate sediments (Walter *et al.* 1993, 2007). It is not clear whether sulphides were present in the Paradoxica Bed at Hunstanton and have subsequently been obscured by oxidation. However, Jeans (1980, pl. 12) has suggested that the corroded coccoliths associated with the Liesegang zones of glauconite staining on the outer surface of this hardground are the result of etching by acids from the oxidation of H_2S.

The main sources of Ca^{2+} for the new cements came from the dissolution of bioclasts made of high-Mg calcite and aragonite as well as Ca^{2+} released from the sediment by acidification as a byproduct of microbial activity. The high Mg-calcite dissolved in the oxic zone, whereas the Sr-rich aragonite lasted longer until within the suboxic zone – it is here that the Sr contents of the cement display an appreciable increase. A plentiful supply of carbonate came from the dissolution of detrital material as well as the HCO_3^- produced by the bacterial oxidation of organic matter. The increasing $\delta^{13}C$ values in the suboxic cement zone suggest an increasing contribution from a source of isotopically heavy carbon. The obvious source is biological methanogenesis, which is unlikely considering the geological situation and the very early phases of marine diagenesis in which these cements were precipitated. The most likely explanation is that the microbes responsible for Mn and Fe reduction in the suboxic zones either selectively oxidized organic substrates with high $\delta^{13}C$ values or their metabolic processes produced isotopically heavy HCO_3^- from normal organic material. Whether the Mn- and Fe-reducing bacteria produce such isotopically heavy HCO_3^- is an open question; it is quite possible that other un-

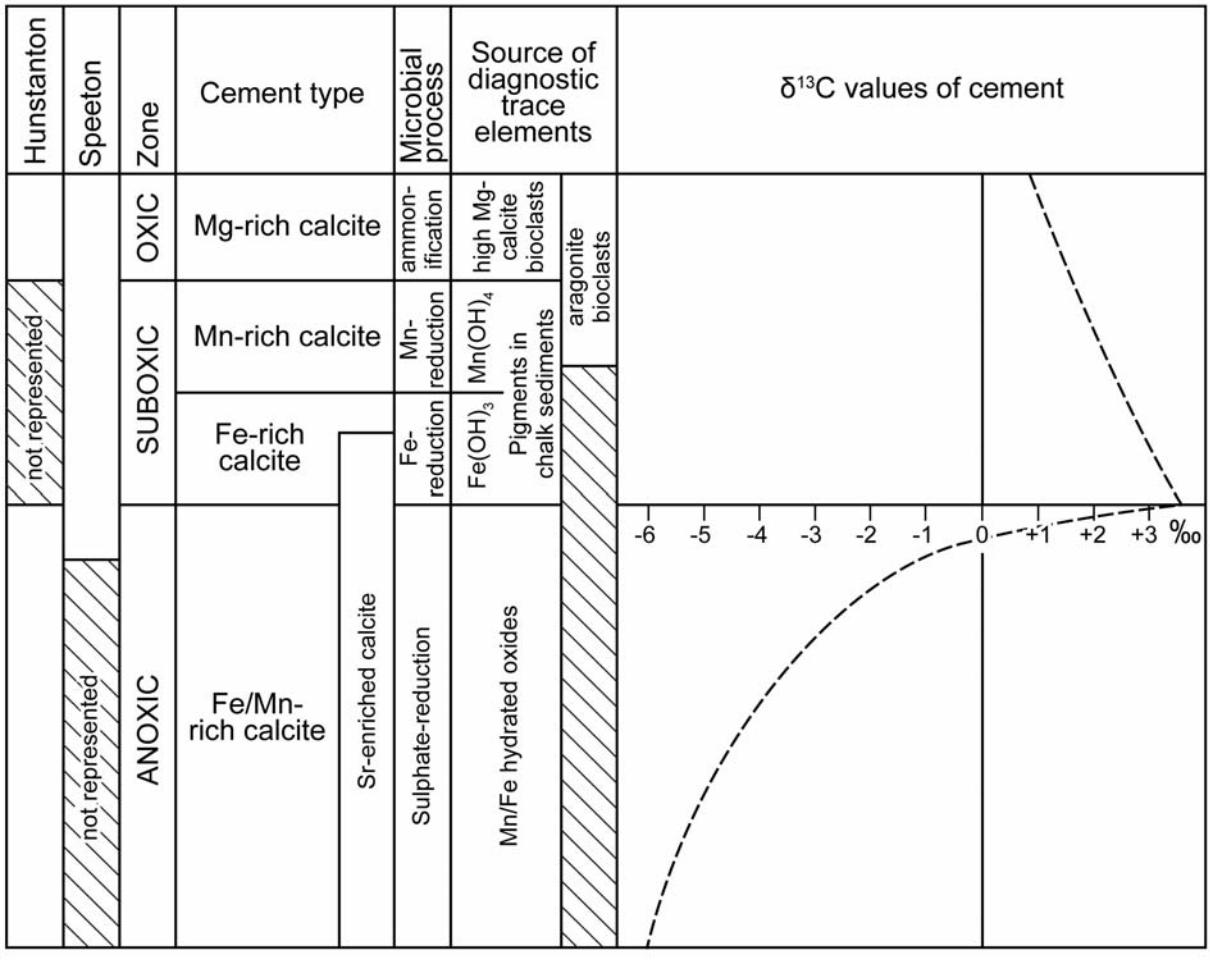

Text-fig. 27. Schematic diagram summarizing the interpretation of the suboxic and anoxic cement series

known microbes may be responsible. The rapid decrease in $\delta^{13}C$ values as the anoxic zone is entered reflects the increasing proportion of HCO_3^- derived from the oxidation of organic matter with $\delta^{13}C$ values ranging from – 20 to –30‰ being involved in cement precipitation during sulphate-reduction.

CONCLUDING COMMENTS

Until now researchers have failed to record directly or deduce indirectly the full sequence of cements that have affected the Upper Cretaceous Chalk. We have side-stepped the direct approach, instead the sequences of calcite cements that are preserved in vugs located in the shell cavities of terebratulid brachiopods have been investigated. These vugs have passively sampled the porefluids and consequently the calcite cements precipitating from them during diagenesis at particular locations and stratigraphical levels within the Cenomanian Chalk of eastern England. Our study has revealed two distinct patterns of cementation that can be related to a variety of early lithifications linked to facies that occur not just in the Cenomanian chalks of eastern England but throughout the Chalk of the UK. Evidence suggests that both were under microbial control and were part of a single pattern of early lithification. Of particular interest is the positive $\delta^{13}C$ trend in the suboxic cement series. As far as we know this has not been recorded in the geological literature. It suggests that the microbes generated heavy $\delta^{13}C$ HCO_3^- which played an increasing role in calcite precipitation as time went on. Such microbes have not yet been discovered. Our approach using brachiopods or perhaps thick shelled echinoids as potential loci of cement-filled vugs, can provide a way to test whether these patterns of cementation are as widespread as they appear to be. Once the nature of the cement sequences are recognized they can be used as a tool for testing a wide range of problems – the study of the cementation history during the development of overpressured oil and gas reservoirs; testing the validity of the $\delta^{13}C$ (calcite) reference curve for the Cenomanian–Campanian Chalk of England as a reliable criterion for intra- and inter-continental stratigraphical correlation (Jeans, Hu, Mortimore, this issue): A time framework to unravel the complex clay mineral assemblages of the Chalk (Hu, Long and Jeans submitted).

Acknowledgements

We wish to thank the following: Vivien Brown for patience and skilfully interpreting handwritten manuscripts; Philip Stickler for drafting figures; Martin Walker for keeping the annular saw working; Chiara Petroni for help with electron microprobe analysis; Mike Hall and James Rolfe for carrying out stable isotope analysis; Tony Fallick and Rory Mortimore for critically reading drafts of this paper and for their helpful comments; and Chris Wood for editorial work. The Chinese Science Council and the Department of Earth Sciences respectively for financial support and hospitality during X.F. Hu's visit (2009–2010) to Cambridge.

REFERENCES

Bower, C.R. and Farmery, J.T. 1910. The zones of the Lower Chalk of Lincolnshire. *Proceedings of the Geologists' Association*, **11**, 333–359.

Brasher, J.E. and Vagle, K.R. 1996. Influence of lithofacies and diagenesis on Norwegian North Sea chalk reservoirs. *AAPG Bulletin*, **80**, 746–769.

Bray, R.J., Green, P.F. and Duddy, I.R. 1992. Thermal history reconstruction using apatite fission track analysis and vitrinite reflectance: a case study from the UK East Midlands and Southern North Sea. In: R.F.P. Hardman (Ed.) Exploration Britain: Geological insights for the next decade. Geological Society, London, Special Publications, **67**, 3–25.

Bromley, R.G. 1967. Some observations on burrows of Thalasinidian Crustacea in chalk hardgrounds. *Quarterly Journal of the Geological Society, London*, **123**, 157–182.

Bromley, R.G. 1968. Burrows and borings in hardgrounds. *Meddelelser fra Dansk Geologisk Forening,* **18**, 247–250.

Bromley, R.G., Schulz, M.G. and Peake, N.B. 1975. Paramoudras: giant flints, long burrows and the early diagenesis of chalks. *Det Kongelige Danske Videnskabernes Selskab, Biologiske Skrifter*, **20**, 1–31.

Clayton, C.J. 1986. The chemical environment of flint formation in Upper Cretaceous chalks. In: G. de G. Sieveking and M.B. Hart (Eds), The scientific study of flint and chert, 43–54. Cambridge University Press, Cambridge.

Craig, H. 1965. The measurement of oxygen isotope palaeotemperature. In: E. Tongiorgi (Ed.), Stable isotopes in oceanographic studies and palaeotemperatures, 3–24. Consiglio Nazionale delle Ricerche.

Dickson, J.A.D. 1965. A modified staining technique for carbonates in thin section. *Nature*, **205**, 587.

Dickson, J.A.D. 1966. Carbonate identification and genesis as revealed by staining. *Journal of Sedimentary Petrology*, **36**, 491–505.

Downing, R.A., Allen, D.J., Bird, M.J., Gale, I.N., Kay, R.L.F. and Smith, I.F. 1985. Cleethorpes No.1 Geothermal Well—a preliminary assessment of the resource. Investi-

gation of the Geothermal Potential of the UK, British Geological Survey.

Egeberg, P.K. and Saigal, G.C. 1991. North Sea chalk diagenesis: cementation of chalks and healing of fractures. *Chemical Geology*, **92**, 339 –354.

Green, P.F. 1989. Thermal and tectonic history of the East Midlands shelf (onshore UK) and the surrounding regions assessed by apatite fission track analysis. *Journal of the Geological Society (London)*, **146**, 755– 773.

Hancock, J.M. 1963. The hardness of the Irish Chalk. *The Irish Naturalists' Journal*, **14**, 157–164.

Hancock, J.M. 1975. The petrology of the Chalk. *Proceedings of the Geologists' Association*, **86**, 499–535.

Hardman, R.F.P. 1982. Chalk reservoirs of the North Sea. *Bulletin of the Geological Society of Denmark*, **30**, 119–137

Holliday, D.W. 1999. Palaeotemperatures, thermal modeling and depth studies in northern and eastern England. *Proceedings of the Yorkshire Geological Society,* **52**, 337–352.

Hopson, P.M. 2005. A stratigraphical framework for the Upper Cretaceous of England & Scotland with statements on the Chalk of Northern Ireland and the UK Offshore Sector RR/05/01. British Geological Survey.

Hopson, P.M., Wilkinson, I.P. and Woods, M.A. 2008. A stratigraphical framework for the Lower Cretaceous of England. British Geological Survey.

Hu, X-F, Long, D. and Jeans, C.V. accepted. A novel approach to the study of the development of the Chalk's smectite assemblage. *Clay Minerals.*

Jeans, C.V. 1980. Early submarine lithification in the Red Chalk and Lower Chalk of Eastern England: a bacterial control model and its implications. *Proceedings of the Yorkshire Geological Society*, **43**, 81–157.

Jeans, C.V., Long, D., Hall, M.A., Bland, D.J. and Cornford, C. 1991. The geochemistry of the Plenus Marls at Dover, England: evidence of fluctuating oceanographic conditions and of glacial control during the development of the Cenomanian–Turonian $\delta^{13}C$ anomaly. *Geological Magazine*, **128**, 603–632.

Jeans, C.V., Hu, X-F, and Mortimore, R.N. 2012. Calcite cements and the stratigraphical significance of the marine $\delta^{13}C$ carbonate reference curve for the Upper Cretaceous Chalk of England. *Acta Geologica Polonica*, **62** (2), 173–196. [this issue]

Jensenius, J. 1987. High-temperature diagenesis in shallow chalk reservoir, Skjolb oilfield, Danish North Sea: evidence from fluid inclusions and oxygen isotopes. *AAPG Bulletin*, **71**, 1378–1386.

Jensenius, J., Buchardt, B., Jørgensen, N.O. and Pedersen, S. 1988. Carbon and oxygen isotopic studies of the chalk reservoir in the Skjolb oilfield, Danish North Sea: implications for diagenesis. *Chemical Geology*, **73**, 97–107.

Jensenius, J. and Munksgaard, N.C. 1989. Large scale hot water migration systems around salt diapirs in the Danish Central Trough and their impact on diagenesis in chalk reservoirs. *Geochimica Cosmochimica Acta*, **53**, 79 –88.

Jørgensen, N.O. 1987. Oxygen and carbon isotope compositions of Upper Cretaceous chalk from the Danish subbasin and the North Sea Central Graben. *Sedimentology*, **34**, 559–570.

Jukes-Browne, A.J. and Hill, W. 1903. The Cretaceous rocks of Britain, Vol. II – the Lower and Middle Chalk of England. Memoir of the Geological Survey of the United Kingdom, London. HMSO, 568 pp.

Jukes-Browne, A.J. and Hill, W. 1904. The Cretaceous rocks of Britain, Vol. III – the Upper Chalk of England. Memoir of the Geological Survey of the United Kingdom, London. HMSO, 566 pp.

Kirby, G.A., Penn, I.E. and Smith, I.F. 1985. Cleethorpes No.1 Geothermal Well: geological well completion report. Investigation of the Geothermal Potential of the UK. British Geological Survey.

Lamplugh, G.W. 1895. Notes on the White Chalk of Yorkshire. *Proceedings of the Yorkshire Geological Society,* **13**, 65–87

Maliva, R.G. and Dickson, J.A.D. 1992. Microfacies and diagenetic controls of porosity in Cretaceous/Tertiary chalks, Eldfisk Field, Norwegian North Sea. *AAPG Bulletin*, **76**, 1825–1838.

Maliva, R.G. and Dickson, J.A.D. 1994. Origin and environment of formation of late diagenetic dolomite in Cretaceous/Tertiary chalk, North Sea Central Graben. *Geological Magazine*, **131**, 609–617.

Maliva, R.G. and Dickson, J.A.D. 1997. Ulster White Limestone Formation (Upper Cretaceous) of Northern Ireland: effects of basalt loading on chalk diagenesis. *Sedimentology*, **44**, 105–112.

Maliva, R.G., Dickson, J.A.D. and Fallick, A.E. 1999. Kaolin cements in limestones; potential indicators of organic-rich pore waters during diagenesis. *Journal of Sedimentary Research*, **69**, 158–163.

Maliva, R.G., Dickson, J.A.D., Smalley, P.C. and Oxtoby, N.H. 1995. Diagenesis of the Machar Field (British North Sea) chalk; evidence for decoupling of diagenesis in fractures and the host rock. *Journal of Sedimentary Research*, **65**, 105–111.

Mimran, Y. 1975. Fabric deformation induced in Cretaceous chalks by tectonic stress. *Tectonophysics*, **26**, 309–316.

Mimran, Y. 1977. Chalk deformation and large-scale migration of calcium carbonate. *Sedimentology*, **24**, 333–360.

Mimran, Y. 1978. The induration of Upper Cretaceous Yorkshire and Irish chalks. *Sedimentary Geology*, **20**, 141–164.

Mitchell, S.F. 1995. Lithostratigraphy and biostratigraphy of the Hunstanton Formation (Red Chalk, Cretaceous) succession at Speeton, North Yorkshire, England. *Proceedings of the Yorkshire Geological Society*, **50**, 285–303.

Mitchell, S.F. 1996. Foraminiferal assemblages from the late Lower and Middle Cenomanian of Speeton (North Yorkshire, UK): relationships with sea-level fluctuations and watermass distribution. *Journal of Micropalaeontology*, **15**, 37–54.

Mortimore, R.N. 2012. Making sense of Chalk: a total rock approach to its Engineering Geology. *Quarterly Journal of Engineering Geology and Hydrology,* **45**.

Oakman, C.D. and Partington, M.A. 1998. Cretaceous. In: K.W. Glennie (Ed.), Petroleum geology of the North Sea: basic concepts and recent advances, 294–349. Blackwell Science, Oxford.

Phillips, J. 1829. *Illustrations of the Geology of Yorkshire*: *Part 1.—the Yorkshire Coast*. 1–192.York.

Plante, A.E. 2007. Soil biogeochemical cycling of inorganic nutrients and metals. In:E.A.Paul (Ed.), Soil microbiology, Ecology and Biochemistry, pp. 389–432. Academic Press.

Rudwick, M.J.S. 1970. Living and Fossil Brachiopods, 1–199 pp. Hutchinson University Library; London.

Sahni, M.R. 1929.A monograph of the Terebratulidae of the British Chalk. Monograph of the Palaeontographical Society London, 1–62.

Scholle, P.A. 1974. Diagenesis of Upper Cretaceous chalks from England, Northern Ireland, and the North Sea. *Special Publication of the International Association of Sedimentologists*, **1**, 177–210.

Starmer, I.C. 1995. Deformation of the Upper Cretaceous Chalk at Selwicks Bay, Flamborough Head, Yorkshire: its significance in the structural evolution of north-east England and the North Sea Basin. *Proceedings of the Yorkshire Geological Society*, **50**, 213–228.

Taylor, S.R. and Lapré, J.F. 1987. North Sea chalk diagenesis: its effect on reservoir location and properties. In: K. Brooks and K.W. Glennie (Eds), Petroleum Geology of North West Europe, 483–495. Graham and Trotman; London.

Walters, L.M., Bischof, S.A., Patterson, W.P. and Lyons, T.W. 1993. Dissolution and recrystallization in modern shelf carbonates: evidence from pore water and solid phase chemistry. *Philosophical Transactions of the Royal Society of London, Series A,* **344**, 27–36

Walters, L.M., Ku, T.C.W., Muehlenbachs, K., Patterson, W.P. and Bonnell, L. 2007, Controls on the d13C of dissolved inorganic carbon in marine pore waters *Deep-Sea Research II*, **54**, 1163–1200.

Watts, N.L. 1983. Microfractures in chalks of Albuskjell Field, Norwegian Sector, North Sea: possible origin and distribution. *American Association Petroleum Geologists Bulletin*, **67**, 201–234

Wolfe, M.J. 1968. Lithification of a carbonate mud: Senonian chalk in Northern Ireland. *Sedimentary Geology*, **2**, 263–290.

Wood, C.J., Batten, D.J., Mortimore, R.N. and Wray, D.S. 1997. The stratigraphy and correlation of the Cenomanian-Turonian boundary interval succession in Lincolnshire, eastern England. *Freiberger Forschungshefte*, **C468**, 333–346.

Wright, C.W. 1935. The Chalk Rock Fauna in East Yorkshire. *Geological Magazine*, **72**, 441–442.

Manuscript submitted: 31th January 2012
Revised version accepted: 25th April 2012